Mathematical Mechanical Biology

Module 3: Biogrowth

Lecture Notes for C5.9

Derek Moulton, Oxford, HT 2020

Based extensively on the notes of Alain Goriely

Contents

HEALTH WARNING:

The following lecture notes are meant as a rough guide to the lectures. They are not meant to replace the lectures. You should expect that some material in these notes will not be covered in class and that extra material will be covered during the lectures (especially longer proofs, examples, and applications). Nevertheless, I will try to follow the notation and the overall structure of the notes as much as possible.

1 Background and motivation

■ Overview

The following section is a general introduction to the problem of growth in biological system. This section will not be covered in class but is included as background material.

Growth is a generic term that describe processes in which the mass of a body changes over time. In biology, the problem of growth is fundamental to all aspects of life from cell-division to morphogenesis, development, maintenance, cancer, and ageing. All life forms experience growth and one of the ultimate challenges of modern biology is to understand how the genetic code is used to transform cells into a fully grown organisms and how such an organism manages to regulate shape and functions through growth and remodelling.

Growth processes also appear in physics to describe problems such as epitaxial growth where new material is fed in the system and reorganised on the substrate. It is also associated with phase transition phenomena where the interface between the phases evolves in time to produce structures such as a crystal [1]. These free boundary problems are controlled by diffusion and unlike problems in biological growth the interface is a line of discontinuity with no particular material property. The swelling of gels is arguably the closest non-biological process that mimics growth as it is non-diffusive and it can be used to test basic mechanical ideas for some biological pattern formation [2].

1.1 Classification of growth

Aspects of growth and remodelling occur during the entire life of an organism. Therefore, growth fills many purposes and functions and, accordingly, is associated with qualitatively different processes. A first classification of growth processes is organised by the way it alters a body, either by mostly changing its volume, its material properties, or the relative position of material points:

Growth. In the modelling of growth, the simple term growth usually refers to the change in mass (typically an increase in mass, but applies obviously to resorption of material as well). This change in mass can be a an addition of new mass at constant density (typical of many soft tissues), a change in density at constant volume (as in the case of a mature bone for instance), or both (as in the case of a developing bone). Mathematically, a theory of growth must take into account the addition of mass either at the boundary of the body or within the body itself.

Remodelling. It is well know that in the process of ageing tissues may get stiffer or softer. The term remodelling refers to the evolution of material properties of a system (typically excluding density), that is the change in time of the stiffness, fibre orientation, fibre strength, and so on. This remodelling process is due to a change in the microstructure that determines the overall behaviour of the tissue. For instance, the typical composition of soft tissues in many animals is a mixture

of collagen fibres within an elastin matrix. Whereas elastin content remains mostly unchanged over many years, there is a continuous turnover of collagen that depends on the local biochemical and mechanical stimuli acting on the cells. The relative content of different types of collagen fibres and elastin determines the overall response of the tissue. This process can occur without change of mass but is nevertheless crucial for the description of a tissue in response to mechanical loadings. From a mathematical perspective, the evolution of material properties can either be modelled by evolving the material parameters of a system or, at a lower scale, by taking properly into account the evolution of different tissue components.

Morphogenesis. Early in embryonic life, new tissues and organs are formed. In this process there is often major reorganisation and differentiation of cells after cell division. Morphogenesis is associated with growth, remodelling, and reorganisation of material elements. This reorganisation process can only happen if the adhesion between different components is weak enough so that they can separate and reattach. This observation has important consequences for modelling as tissues undergoing morphogenesis exhibits rapid elastic stress relaxation and plastic-like flow. In many instances, it may therefore be more appropriate to describe such tissues or collections of cells as a fluid or as a visco-elastic material rather than an elastic material with evolving configuration.

Further, growth itself can be classified by the location of growth and the manner in which new material is added to the existing structure. The main categories are: tip growth, accretive growth, and bulk growth as describe below.

1.1.1 Tip Growth.

First described by Duhamel du Monceau in 1758 [3] for the growth of roots, *tip growth* (or *apical growth*) describes growth processes that take place in a small region at the tip of filamentary structures (See Fig. 1). It is the main growth mechanism used microbial organisms and plant systems such as fungi, filamentary bacteria, pollen tubes, or root hair. Since growth occurs in a region of constant size, the overall scaling of mass with time is linear. This linear scaling is avoided by allowing branching, a typical features of these filamentary systems, that allows for essentially one-dimensional structures to explore a three-dimensional volume for nutrients. Tip growth is sometimes referred to as *primary growth* in plants. Indeed, once a stem or root is large enough, it will also be subject to secondary growth by thickening through the addition of external layers. Mechanically, the problem of tip growth is to understand the interaction of the tip with its environment, its shape, width, internal stresses, and how it evolves based on laws of material addition within the walls.

1.1.2 Accretive Growth.

Accretive, *surface*, or *appositional growth* describe mechanisms such as deposition in hard tissues where new material is added to the boundary of an existing body. It is the typical mechanism responsible for the formation of teeth, seashells, horns. At

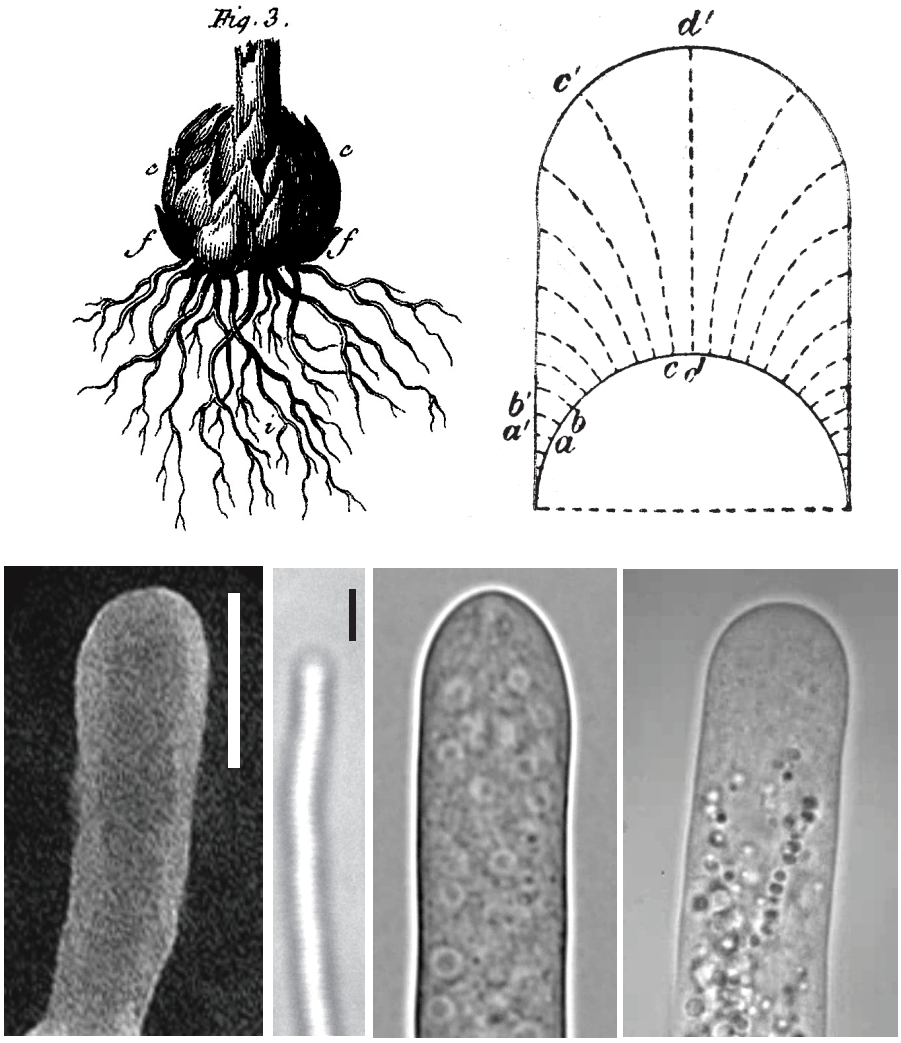

Figure 1: Top row. Left: Growing root as depicted by Duhamel in 1758 [3]. Right: First theoretical description of tip growth by Reinhardt in 1892 for the growth of fungus [4]. Bottom row: pictures of growing tips. From left to right: actinomycetes from a spore, bar is 1μm (source: Society for Actinomycetes Japan.); *streptomyces* A3(2), bar is 1μm; *allomyces*; lily root hair (typical diameter 15-20μm) (images courtesy of J. Dumais).

the microscopic level surface growth is also found in bones where changes in bone density occur by deposition or resorption of new material on the surface of trabeculae or the walls of canals excavated by osteoclast [5]. Mathematically, many problems in accretive growth can be modelled by assigning an accretion vector at the boundary of the body based on the local geometry (See Fig. 2). The problem amounts then to evolve that boundary based on the accretion vector and recompute the new shape to obtain the information on the local geometry necessary to further evolve the system. The key question from a modelling point of view is to obtain an accretion law from the interaction of the soft tissue of the animal with the new accreted part and evolve, accordingly, the hard body.

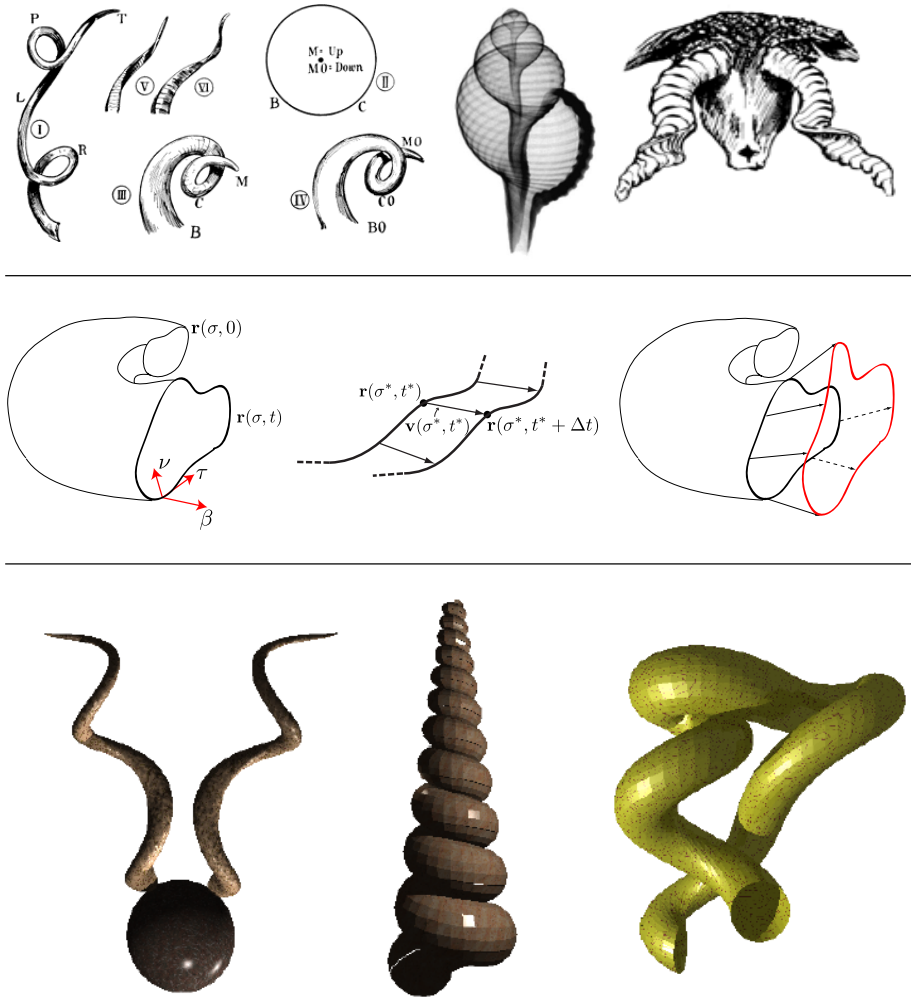

Figure 2: Accretive growth. Top Row: Growth of horns and seashells as described by D'Arcy Thompson [5]. Middle row: The theoretical basis of accretive growth. For a given body at time t, an accretion vector is defined at the active growth boundary. At time $t + dt$ a new surface (in red) is created. Bottom row: different body forms obtained by different choices for the accretion vector (from [6]).

1.1.3 Bulk growth.

Bulk, *volumetric* or *interstitial* growth refer to processes in which local volume elements in the material change over time (rather than on the boundary of the body as in accretive growth). It is typical of many developmental, physiological or pathological processes and has been particularly well documented in specific systems such as arteries, heart, muscles, and solid tumours. Bulk growth encompasses *hyperplasia*, the increase of volume due to cell proliferation typical of many developmental systems; *hypertrophy*, the change of volume due the enlargement of its constituents, typical of many physiological processes; and *neoplasia*, the abnormal and often unregulated growth or division of cells, typical of tumour growth. Mathematically, bulk growth offers many interesting challenges. First, a local volume element may not remain isotropic during growth and a tensorial description of growth is therefore needed. Indeed, imagine a small sphere with a given set of axes. In an anisotropic growth process this small sphere will be transformed into an ellipsoid with a new set of principal axes. The mapping in Euclidean space that describes this local transformation maps the axes of the initial configuration of the sphere to the principal axes of the ellipsoid and it is fully described by a tensor, the *growth tensor*. A second challenge in bulk growth is that it applies to soft tissues that are elastic. Therefore, it is not clear if the deformation observed from an initial state is due to the growth or the elastic response of the material, or both. This problem which will be discussed at length in this review was first formulated by Hsu in 1968 in what may be considered as the first work to address the problem of mechanical growth modelling: "*If the form to which a body grows under no applied loads is known, what will be the form of the body if some mechanical loads are applied during its growth?*". Note that from a modelling perspective, bulk growth can be used to described the growth of filamentary objects (for instance neurons or plant stems which have distributed growth) or surfaces (such as layers of cells which do not change their thickness).

The classification of growth as tip, accretive, and bulk is, are not rigid and depends on the scale at which the problem is being studied. Indeed, both tip growth and accretive growth could be modelled as bulk growth processes where a thin soft layer close to the boundary expands and stiffens in time rather than new material being added at the boundary. Indeed, tip growth is a bulk process that is localised at the apical part of the filament and a detailed analysis of this process requires an understanding of areal growth due to insertion of new materials in the apical zone. Similarly, bone growth and wound healing can be seen either as an accretive process or a localised bulk process where density evolves.

1.2 The scaling of growth

The first question to be addressed when thinking about growth concerns the evolution of the mass of an organ or an organism with respect to time. If both total mass of an individual and the mass of an organ is known, we can naturally ask how an organ evolves relatively in comparison to the organism. For isntance, one can ask: how does the brain grow with respect to the total weight? How does height scale with weight? and so on. Despite the fact that the total mass M is the only objective

measure of size applicable to all biological organisms, the first historical records of growth evolution was on the height of human. In 1759, Count Philibert Gueneau de Montbeillard started to record every 6 months the height $H(t)$ of his son from his birthday to the age of 18. This record shown in Fig. 3 was published in the fourth volume of the supplement to Buffon's "Histoire Naturelle" [7]. The first complete

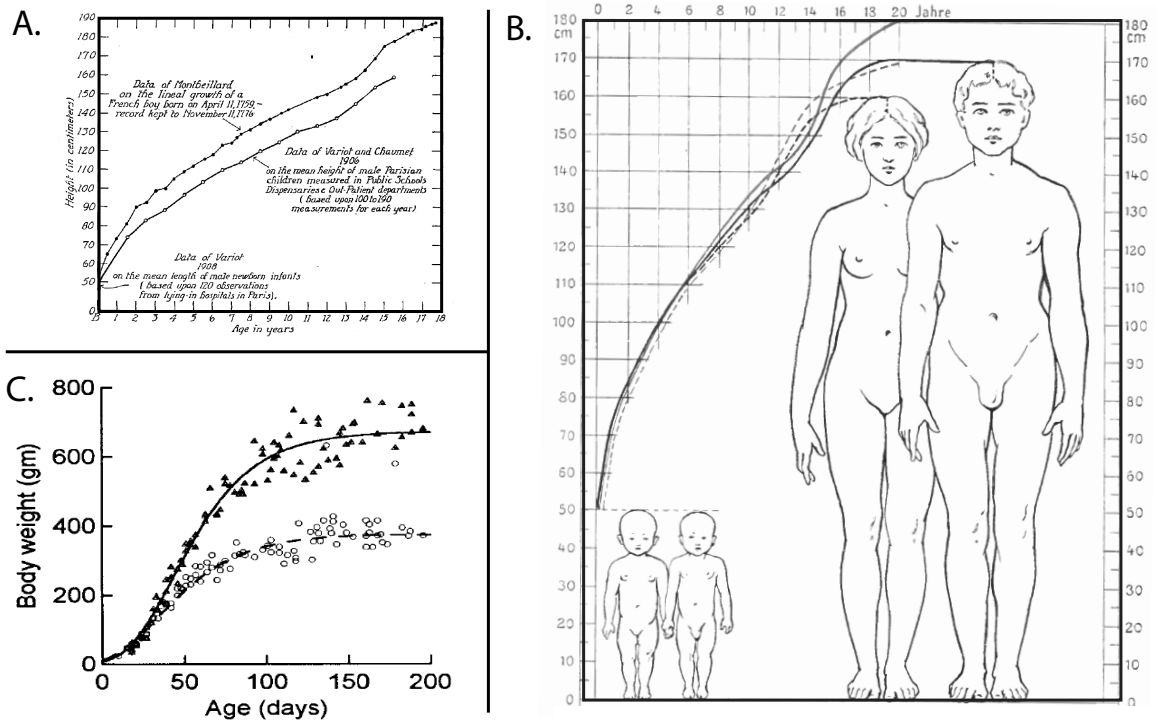

Figure 3: The growth of man (and rats). A. First record of longitudinal growth done by Count Montbeillard in 1759 (reproduced from [7]). B. Growth curves from Stratz's book in 1904 [8] and C. Growth curves for rats fitted by a Gompertz law [9].

.

statistical study of the evolution of weight and height in man was conducted by the Belgian polymath Adolphe Quetelet and published in 1835, in his "Treatise on Man" [10]. In this remarkable book, Quetelet pooled and analysed data from the Belgian population and considered both general trends and deviations around average by use of the Gaussian distribution (which is considered to be the first use of the Gaussian distribution for a statistical study). Quetelet also suggested a law of growth by fitting the data of height $H(t)$ against time t by

$$H(t) = at + \frac{b+t}{1+\frac{4}{3}t}, \tag{1}$$

and a scaling of weight versus height of the form $W = cH^{\alpha}$ where $\alpha = 5/2$ during development and $\alpha = 2$ for adults, in which case the Quetelet coefficient c becomes the infamous Body Mass Index, which remains a critical estimate of fitness and obesity despite its obvious shortcomings and many criticisms [11]. The attempt to scale height with respect to weight also represents one of the first attempts to obtain an allometric

law in biology, that is a power law between a given physical quantity and the total mass of the organism [12].

By the end of the nineteenth century there was a flurry of activity dedicated to understanding both the growth of humans by itself but also in comparison with the growth of animals and plants [13]. The idea emerged that up to a rescaling of time and mass, growth in different biological organisms could follow some universal laws. Many of these studies are well described in the seminal book by d'Arcy Thompson on "Growth and Form" first published in 1917 [5].

Bogin reports that by 1972 no less than 200 different models or fitting functions had been proposed to describe the evolution of human growth [14]. The first attempt to model the evolution of the total mass based on physical principles relies on an idea by Pütter [15] first published in 1920. Pütter proposed that animal growth can be seem as a balance between addition and removal of building materials in the body. Growth proceeds as long as new material is added faster than it is removed and stops when both processes are balanced.

Mathematically, the rate of material removal is typically assumed to be proportional to the mass $M(t)$ itself as in a standard decay problem whereas the rate of addition of new material is proportional to a power of the mass which leads to [16]

$$\frac{dM}{dt} \equiv \dot{M} = M(aM^{-p} - b), \tag{2}$$

where $a, b > 0$, $0 \leq p < 1$ and $M_\infty = (a/b)^{1/p}$ is the asymptotic mass. If $M_0 = M(t = 0)$ is the mass at birth, the solution of this equation is $M(t) = M_0 \mathrm{e}^{(a-b)t}$ if $p = 0$ and

$$\left(\frac{M(t)}{M_\infty}\right)^p = 1 - \left[1 - \left(\frac{M_0}{M_\infty}\right)^p\right] \mathrm{e}^{-bpt}, \tag{3}$$

otherwise (See Fig. 4B for an example with $p = 1/4$). Note that Eq. (2) also contains the classical logistic curve [17] in the limit $p \to -1$ with a and b negative and Richards model [18] (with $p < -1$, a and b negative) used to model the growth of plants.

The choice for the exponent p is more problematic. A typical argument is to assume that the addition of new material is limited by energy input and metabolic rates. It the energy intake and growth rate are directly proportional to the weight itself, we have $\dot{M} \sim M$, that is $p = 0$, and exponential unlimited growth is expected. This behaviour observed in the early developmental stages of insects is only valid until a change in the mode of growth takes place.

If we assume that the metabolic rate follows a scaling based on geometry and that energy intake is proportional to the surface area, we have $\dot{M} \sim M^{2/3}$, that is $p = 1/3$ (a power law originally proposed in 1839 by Sarrus and Rameaux [19]) but, more generally, Ludwig von Bertalanffy [16] suggested that most biological systems grow in an intermediate regime with exponent $0 < p < 1/3$.

More recently, it was proposed [20] that the production of new material should be related to Kleiber's law [21] that states that the metabolic rate of an organism (defined as the energy expended by an organism per unit time) scales as the 3/4 power of the total mass (See Fig. 4C) leading to $p = 1/4$. It has been argued that this power law for metabolic rate is widely applicable to biological systems perhaps over 27 orders of

magnitude from bacteria to whales and even plants and forests [22], but many have also criticised the validity of such statistical analysis and have argued for exponents closer to 2/3 [23]. The origin and justification of this type of power laws in terms of first principles have remained elusive. Unfortunately, the lack of scientific theory is naturally fuel for endless discussions, debates, opinions, and controversies with very little mathematical content and the general field of scaling laws for growth has confused motion for progress [24].

For any choice of exponent $p \in]0, 1]$, these growth curves show a sigmoidal behaviour (See Fig. 4B) that is indeed observed in many systems. This sigmoidal behaviour describes well a slow initial phase followed by quick maturation, ending with an asymptotic limit typically describing an organisms after its reproductive phase (note also humans have evolved and adapted in such a way as to avoid many power laws applicable to many species including the simple law (2)). Nevertheless, human growth can be modelled by considering pre-pubertal and post-pubertal periods as separate [25]).

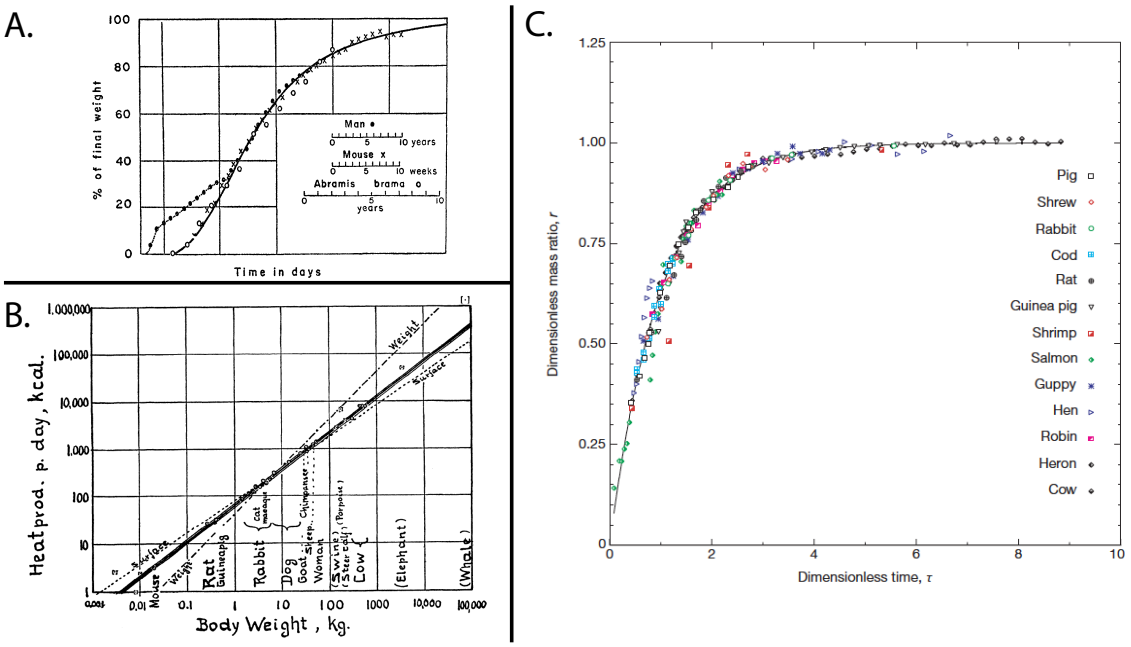

Figure 4: Growth laws and scaling. A. Growth evolution from von Bertalanffy [16] . B. Kleiber's law: Metabolic rate as a function of mass [21]. C. Scaling and data analysis based on Kleiber's law (From [20]). Here M/M_∞ is plotted agains the dimensionless time $\tau = bpt - \ln(1 - (\frac{M_0}{M_\infty})^p)$ as described by Eq. (3) with $p = 1/4$.

The key feature of this simple model is that it identifies the *specific growth rate*[1] given by $\dot{M}/M$ as a central quantity. Indeed, the basic idea is that a proportion of new tissue generated by growth is capable of growing itself but as time goes by, this ability is reduced. These two principles were well described by Peter Medawar [26] who

[1]The term specific is correct here as it refers, in general, to a quantity per unit mass.

wrote:"*What results from biological growth is itself, capable, of growing*" and "*Under the actual conditions of development the specific acceleration of growth is always negative*".

Another possible law that has been used in the context of growth is the Gompertz law, first introduced in 1825 [27] for the evolution of human population, then used in actuarial sciences as a modified compound law, then proposed as a suitable growth law for organisms [28]. The Gompertz law is obtained as the solution of a Malthusian equation of growth $\dot{M} = KM$ with a growth rate K decaying exponentially in time

$$\dot{M} = ae^{-kt}M, \qquad a = k \ln\left(\frac{M_\infty}{M_0}\right), \tag{4}$$

which leads to

$$M(t) = M_\infty \left(\frac{M_\infty}{M_0}\right)^{-e^{-kt}}. \tag{5}$$

This rather unfriendly mathematical equation (whose solution contains the exponential of an exponential and two characteristic time scales) has been shown to be a particularly good fit for bacterial and tumour growth among others [29] and remains widely used for fitting data (See Fig. 3B).

1.3 Relative growth

Psychological studies have shown that children are undeniably cute and loveable [30]. It has been argued that this cuteness factor, a propensity or desire to cuddle or defend a person, is due in part to our perception of the relative size of body and facial features in children versus adults [31]. Proportionally, the skull of babies is larger than the ones of adults (See for instance Fig. 5) [32] and further relative dimensions of the skulls (height versus diameter, roundness) also evolve. Indeed, no adult organism is a pure dilation of itself at birth. The case of a pure dilation of any organ from initial to adult life is referred as a case of *isometric growth* whereas the relative growth of an organ with respect to the total weight of the organism is known as *allometric growth* [33]. Therefore, the second natural problem of growth that follows from the studies of mass evolution is to understand how organs, limbs, or tissues grow with respect to the total body mass, the general topic of *relative growth*.

The subject of relative growth developed at the end of the 19th century with the early work of Dubois and Lapicque on the relative size of the brain in different species [37] and within a given species [38] following an early observation from Cuvier that bigger mammals have relatively smaller brains [39]. Following extensive work on various aspects of differential growth by D'Arcy Thompson [5], the subject was further expanded and applied to many different biological systems by Julian Huxley in his book "Problem of Relative Growth" [40] where he coined the word *allometry* to describe relative growth that follows a power law.

The central idea in Huxley's work is that the mass m or length l of an organ scales as a power of the total mass M of the organism, that is

$$m = kM^\alpha. \tag{6}$$

Note that by expressing m as a function of M, one removes the explicit dependence on time which allows to consider only the size m and M at a given points of development

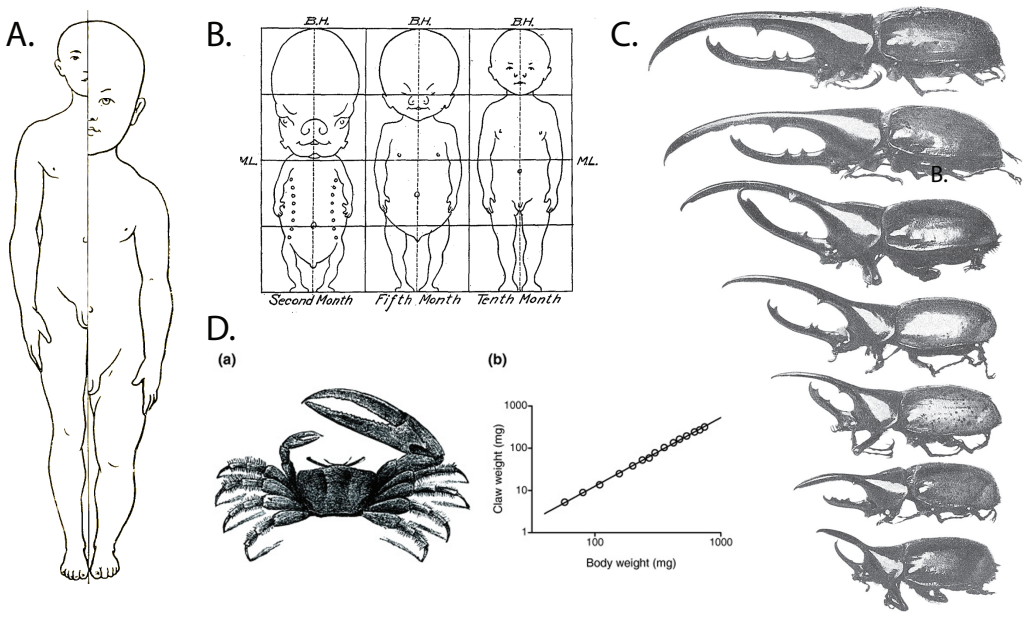

Figure 5: Relative growth. A. and B. Relative proportion in the growth of man (from Stratz [8]) C. Allometric scaling for the claw of the fiddler crab (from [34]). D. Different males *Dynastes* showing the relative increase of horns as a function of size. Illustrations from Champy 1924 [35] (Reproduced from [36])

.

when making comparisons between animals. If masses are compared, the case $\alpha = 1$ corresponds to isometric growth and any other exponent would be considered as relative or allometric growth. If this scaling also holds during growth (that is both k and α are time-independent), it simply states that the two specific growth rates of an organ and an organisms are proportional, that is

$$m = kM^{\alpha} \quad \Longleftrightarrow \quad \frac{\dot{m}}{m} = \alpha \frac{\dot{M}}{M}. \tag{7}$$

Starting in the 1920's, this simple but fundamental idea has played the role of an ordering principle in comparative biology and evolution [41]. The possibilities are endless as the size of any organ in any species can be compared to any other ones from any other species at any point in the development and generations after generations, students and researchers in biology have combed the beaches, swept the forests, and fished the seas to gather data on size and weight. Typically, one compares either the relative size of different organs in one species (*intraspecific allometry*), the relative sizes of one organ within different species (*interspecific allometry*), or the relative size of one organ or different organs at different point in development for a given species (*dynamic allometry*).

A typical allometric study proceeds with the following steps *(i)* gather experimental or bibliographic data on either the size of an organ or the metabolic rate of an organism and its total weight in different species; *(ii)* plot this data in a log-log plot; *(iii)* find the best linear fit and extract the slope α; *(iv)* Find a simple rational number close

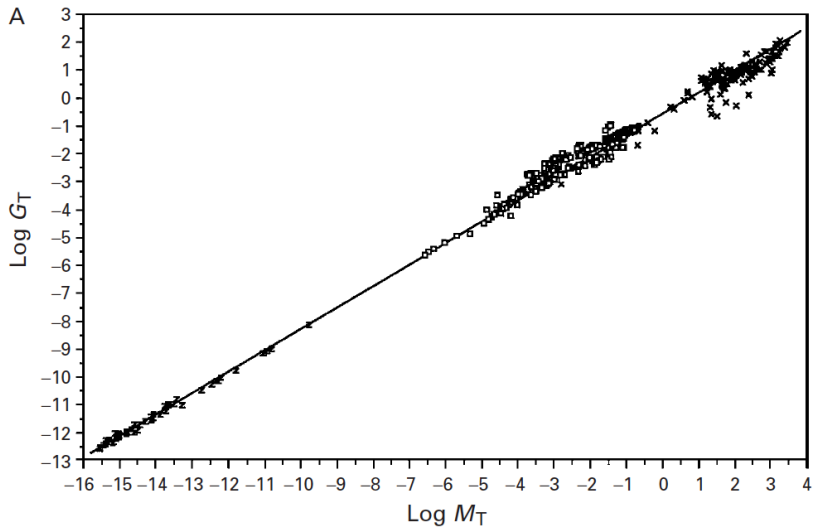

Figure 6: Allometry in plants. An interesting example of a possible allometric law for growth arises in plants when the growth rate is plotted against the weight [22].

.

to α and argue on geometry, physics, network theory, or thermodynamics ground that this slope was predicted from simple first principles; *(v)* discuss the relevance of this new law of nature in the context of physiology, pathology, or evolution; *(vi)* discuss why some species or organs may not follow the expected law, hence justifying the rule through its exceptions [42]. Fig. 6 shows an example of growth rate allometry in plants. These studies, despite their obvious shortcomings from a epistemological point of view, have been incredibly successful and power laws nowadays are the very few quantitative laws related to shape and size that seem to hold across diverse organisms [43]. As such, allometry remains nowadays a favourite tool and a methodological framework for comparative biology [44]. More importantly, for the study of growth, the mere existence of observed scaling laws, that is the undeniable fact that aspects of sizes, growth rates, or metabolic rates tend to cluster in a linear fashion against total weight when expressed in log-log coordinates, suggest that critical aspects of size and growth rate are indeed governed or constrained by geometry, mechanics, and physics as already argued by Medawar in 1941 [26][2].

At the organ or body level, relative growth can be measured by direct measurement. However, organs themselves do not follow necessarily isometric growth and experience different growth rates at different points. The skull of mammals typically elongate after birth, brains in humans fold onto themselves during development, and roots tend to grow by limiting their growth in a small region at the tip. Growth, typically is neither isometric nor homogeneous. Therefore, when studying growth it is important to consider that different points on the growing body may grow at different rates creating, in the words of Huxley, *growth gradients* and *growth sources* [40], and in the terminology preferred by 19th century plant physiologists *differential growth* [45]. Differential growth is central to all aspects of growth mechanics as it is responsible not only for

[2]Note however that Medawar believed that growth is dominated and limited by diffusion, which turns out to be relevant only at the microscopic scale.

shaping an organism but also for creating stresses through geoemtric incompatibility. However, to capture its key features new experimental and mathematical methods are needed.

1.4 Stress influences growth

From a biologist perspective growth is mediated by gene activation and regulation. In a simplified view, different genes will trigger different growth responses. For instance, in the case of the leaf of the model plant *Arabidopsis thaliana*, a number of genes and microRNAs have been identified that regulate and control the shape of leaves during development (See Fig. 7). Exquisite details are known on the initial stage of leaf formation including features such as adaxial-abaxial polarity, symmetry, and flat morphology, as well as the precise control of cell division, proliferation and expansion. This genetic

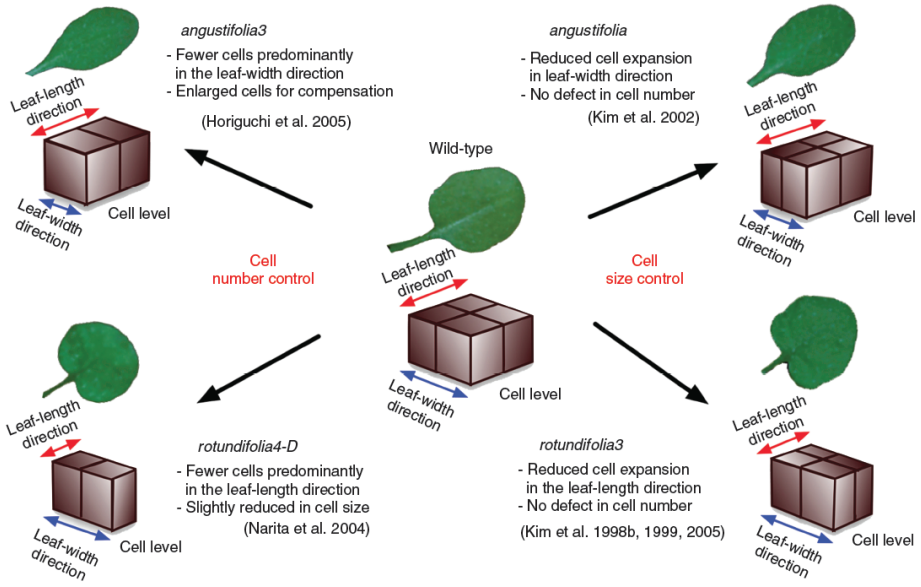

Figure 7: A genetic view of growth. The shape and size of a leaf is determined during development by a number of regulatory genes that have been identified by systematic genetic studies [46].

.

perspective of growth is fundamental as it identifies at the smallest scale the essential features that control cell division and expansion. It also provides information at the local level on the change in shape and volume of the growing components of a body. Nevertheless, a leaf will only acquire a shape as a result of cell division by developing physical forces between cells or within a cell. There are important physical, geometric, and mechanical constraints in the development of a tissue or an organ that need to be integrated with genetic and biochemical signals to obtain a full picture of growth.

The fact that mechanical loading has an effect on growth is not surprising as many anecdotical facts are well appreciated. We know, for instance, that muscles will grow when repeatedly strained during exercise. We know also that astronauts will loose bone mass in space flights due to the effect of reduced gravity [47] and, conversely, that

tennis players have denser bones in their playing arms [48], that trees will grow shorter but more stubby in areas which are more windy [49], that the earlobe will stretch and grow under the action of heavy earrings and that foot-binding results in smaller foot size and permanent deformations [50]. The precise nature of how mechanical signals applied in the bulk or at the boundary of a body are mediated down to the cell and the nucleus is not yet known but the effect of the mechanical environment on the regulation of growth is undeniable.

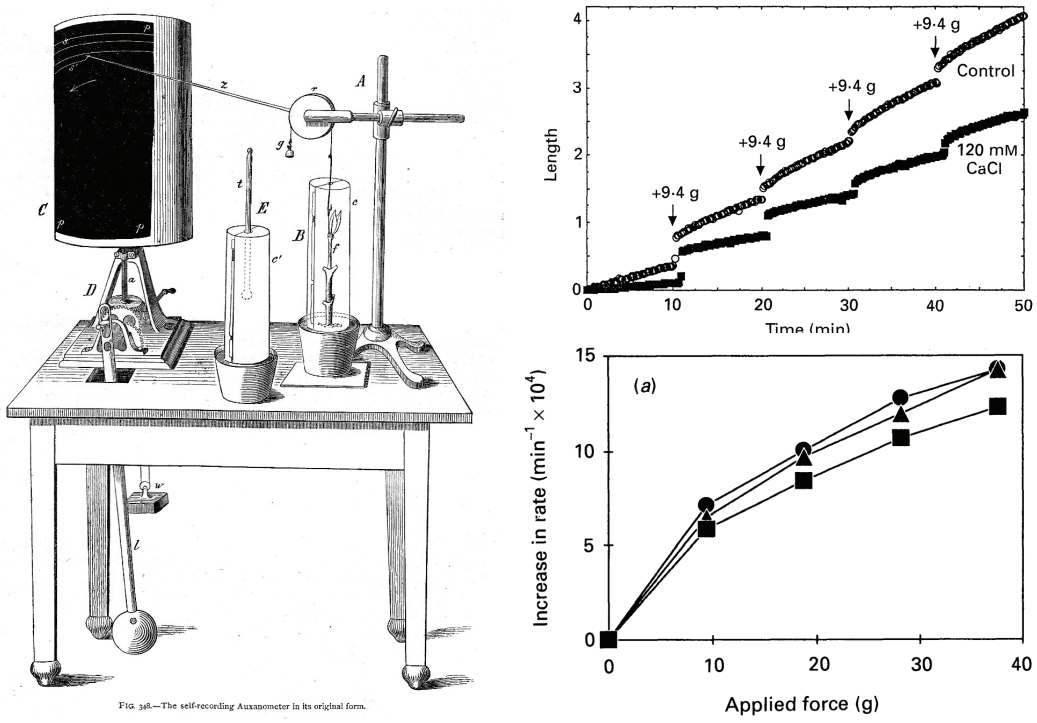

Figure 8: A mechanical view of growth. Left: The length of a growing stem is continuously recorded while the plant is being pulled by different weight (from Sachs's Text-book of botany [45]). Right. Results of a similar experiments performed on maize leaves. Different weights are being attached leading to different growth velocity and growth rate as a function of the applied force [51].

.

The influence of stress and mechanical loading on growth and physiological regulation is well documented in many systems some of which we briefly review next.

1.4.1 The growth of stems

Simple experiments that quantified the relationship between growth and applied stress were already performed by plant physiologists of the 19th Century. The idea is as simple as it is beautiful. As a stem grows, a string is attached to its tip and tied around a pulley (See Fig. 8). Different weights can be placed at the other end of the string to apply different constant forces to the growing stem. The length of the stem is continuously recorded by an auxanometer. Experiments on maize leaves show that the

growth rate increases with the applied load demonstrating very clearly the relationship between external loading and growth.

1.4.2 The growth of axons

Another interesting example of stress-mediated growth in a biological system is found in the development and branching of neurons. Most neurons have a very distinctive morphology with a large cell body and long protoplasmic protrusions from the cell body. These protrusions, called *neurites*, develop into either axons or dendrites that connect to each other to create a connected network, the nervous system. The initiation, development, and growth of axons have been shown to depend on applied mechanical forces [52]. The initiation of axons of chick sensory neurons, chick forebrain neurons and rat PC12 cells can be experimentally manipulated by the proper application of tension on the surface of the cell body [53]. Following initiation, the elongation of an axon can be manipulated by first gluing a calibrated glass needle and then towing the neurons with constant force leading to different growth rate (See Fig. 9).

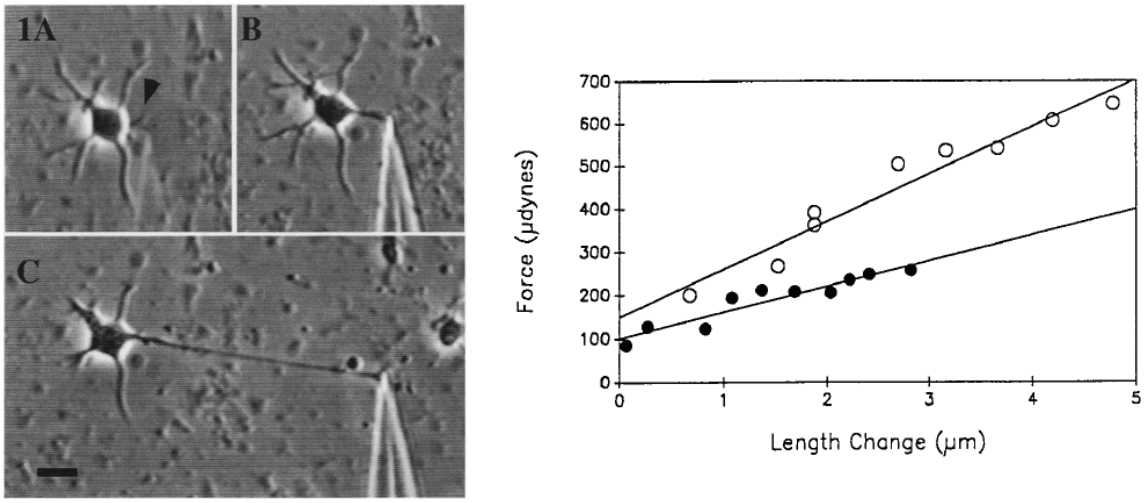

Figure 9: Growth of an axon: Right: Experimental elongation of a neurite in a stage 2 hippocampal neuron induced by applied tension. (A) Neuron immediately before needle application. Arrowhead marks position to which needle was attached. (B) Same neuron 30 min later during early stage of neurite towing. (C) 5:40 h/min after panel B, at the end of towing. Bar, 20 μm.[54] Left: Axonal elongation rate for chick sensory neurites as a function of experimentally applied tension. Each line reflects the data of single towed neurite. Data and graphs from [55].

1.4.3 Thoma's law in arteries

Arteries are the blood vessels that carry blood from the heart to organs and body tissues. Mechanically, they can be seen as mostly cylindrical structure with a triple layer of visco-elastic material that can grow and remodel. The arterial system is a highly complicated and regulated mechanical system sustaining varying pressures, loads, and

stresses. It has been known since the early work of R. Thoma in 1893 ([56], see also [57, 58]) that the magnitude of blood flow in chick embryo blood vessels regulates the vessels' diameters and further that this effect is mediated through shear stress on the inner arterial wall. Thoma also showed that the magnitude of pressure regulates the vessels' thicknesses. These observations on mechanical regulation of artery thickness and diameter have been verified experimentally over the years [59]. Arteries also respond to changes in axial loading; a sustained increase in axial loading tends to lengthen arteries in culture and in vivo suggesting that axial stress (or strain) is also regulated towards a homeostatic value [60].

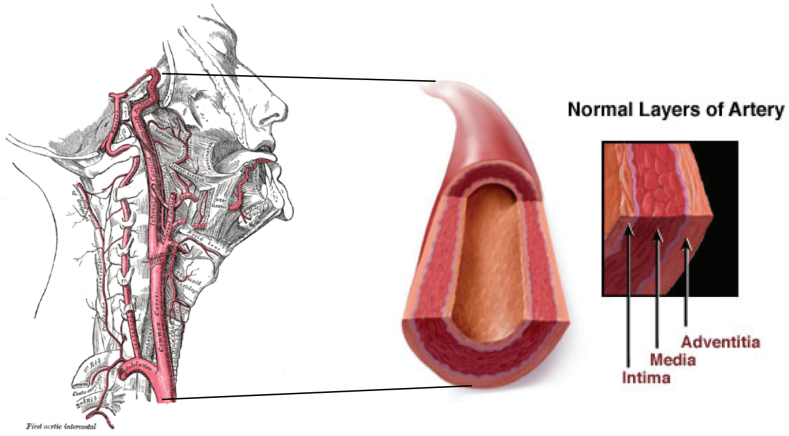

Figure 10: Arteries are the main blood vessels in the body carrying blood from the heart to organs and body tissues. Their thickness, diameter, and length are regulated by mechanical stimuli, among others.

1.4.4 Woods law for the heart

The heart is a complicated organ that pumps blood to the body by active muscular contraction. The heart size and thickness is regulated during homeostasis to maintain proper function. In 1892 Woods proposed that wall stress is a key factor in this regulation process [61]. The basic idea of Woods is to look at the heart as an elastic membrane and use Laplace's law to obtain information on wall stresses (See Fig. 11). Laplace's law (sometimes called Young's law or Laplace-Young's law [62]) states that for an elastic membrane, the difference of pressure P accross the membrane is related to the principal curvatures κ_1 and κ_2, the wall thickness h and principal wall stresses by

$$P = h\left(\sigma_1\kappa_1 + \sigma_2\kappa_2\right). \tag{8}$$

If we assume transverse isotropy of the walls, we obtain $P = h\sigma(\kappa_1 + \kappa_2)$. Woods showed through direct geometric measurement that the ratio

$$C_{\text{Woods}} = P/\sigma = h(\kappa_1 + \kappa_2) \tag{9}$$

is nearly constant across the heart. More strikingly, the Woods number C_{Woods} also seem vary only by about 22% across different mammal and birds species [63]. The

idea is then that wall stress could be the prime regulator of heart size and thickness. In simple terms, Woods' law states that the heart grows and remodels as to keep wall stress constant. This law is consistent with various pathologies and regulatory mechanisms. For instance, during long periods of high blood pressure P due to pathological conditions, the heart ventricles thicken by addition of myofibrils as to lower wall stress over long time. Similarly, athletic exercise leads to increase in volume loading that decreases the curvature κ of the heart and will be matched by an increase in muscle fibre length that will also increase the heart thickness h.

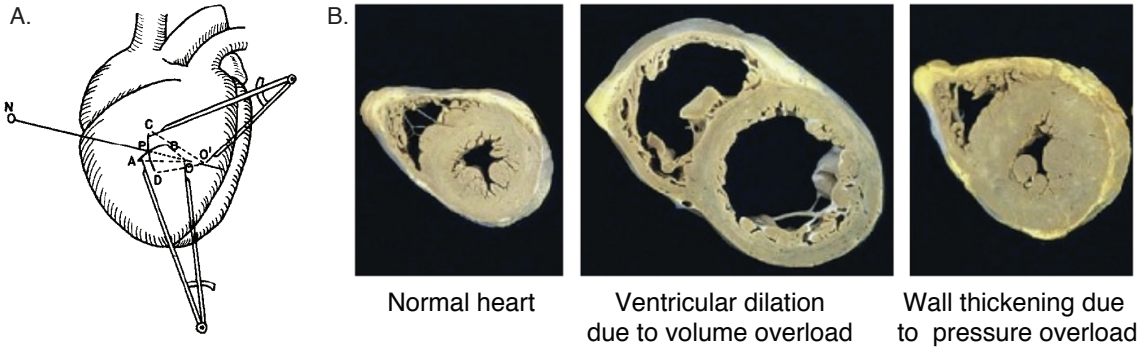

Figure 11: Growth and remodlling in the heart: A. Observation of the principal radii of curvature on the hear surface as originally performed by Woods [64]. (B) Pathology of the heart leading to increase in size. Left: normal heart, middle: ventricular dilation due to volume overload, right: increase in wall thickness due to pressure overload [65] Reproduced WITHOUT permission.

1.4.5 Tumour spheroid growth

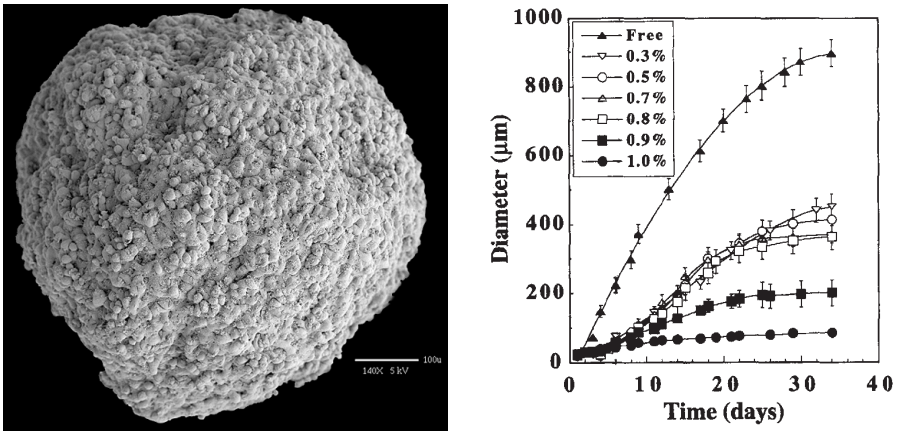

Figure 12: Multicellular tumour spheroids. Left: three-dimensional structure (bar is 250 mm) reproduced WITHOUT permission from [66]. Right: Growth kinetics of spheroids grown in agarose gels of different concentration showing that as the gel gets stiffer the asymptotic size of the spheroid is smaller. Right: Geometry of the problem

Cancer cells can be cultured *in vitro* to grow on a gel or in a pool of nutrients and form a sphere-like shape, *a spheroid* [67] (See Fig. 12). These spheroids are of great interest as they can be used in a variety of settings to understand the response of cancer cells under different physical, chemical, and genetic treatments [68]. Mathematically, the delightful spherical symmetry of these aggregates allows for a direct comparison to experiments and a reduction of the problem difficulty by only considering the evolution of the spheroid radius [69]. The fact that tumour growth is related to mechanical stresses was nicely demonstrated by Helmlinger *et al.* who showed that the final size of the spheroid depends on the concentration of the agarose gels in which it is cultured [70]. This study suggest that solid stress (among other factors such as nutrients and acidity) has a direct effect on growth as high stress may limit the ability of cells to divide through contact inhibition [70].

1.5 Growth influences stresses: the problem of residual stress

Wapas, Walapas, or Walabas are the generic names for trees belonging to the genus *Eperua*. They are found through French and British Guyanas where they are the most abundant tree species. These trees grow rapidly and can be cut every 30 years, representing an important economic resource [71]. However, despite their abundance and rapid growth, Wapas are not widely exploited as they are also locally called: "les arbres tueurs" (the killer trees), for the danger associated with harvesting them as they often burst open as they are cut, presenting a real danger for workers [72]. The tendency to burst is a perfect and extreme example of the release of residual stress in plants, what plant physiologists call *tissue tension* [73]. In many biological tissues, due to a combination of cellular, chemical, and mechanical factors, different parts of the tissue experience different growth rates. The net result of this *differential growth* is that the tissue may be under stress even when unloaded. *Residual stress* is the stress field that may exist in a body when unloaded. The generation of residual stress through differential growth is the a critical feature of any mechanical theory of growth [74]. Essentially, as growth takes place locally, parts of the body need to be stretched or compressed to ensure integrity (no cavitation) and compatibility (no overlap) of the body. In turn, the strains associated with these residual stresses are referred to as *residual strains* [75].

A smaller and simpler experiment to visualise and demonstrate tissue tension in plants can be done in the kitchen with a stalk of rhubarb (*Rheum rhabarbarum*) and a kitchen peeler [77, p. 47]. A stalk of rhubarb is made up of an outer layer consisting of the epidermal tissue and the collenchyma layers, and an inner layer consisting chiefly of parenchyma. If you carefully peel a strip of the stalk's outer layer and attempt to place it in its original position, you will notice that the strip has shrunk in length by about 2%. If you peel the other outer layers, you may realise that the inner part (the *pith*) is extending in length (by about 6%). This simple experiment shows that the outer wall is in a state of axial tension while the pith is in a state of axial compression (See Fig. 14). The possible mechanical role of these stresses and combination of tissues can be appreciated by realising that the peeled rhubarb has lost most of its rigidity; so much so that it now buckles under its own weight. Similarly if the rhubarb is cut along its axis, it will tend to bend outwards as part of the elastic stress is relieved when the

Figure 13: Right: *Eperua venosa.* Wapas are trees that burst when cut as a result of their rapid differential growth causing residual stress. Top Left : When they are cut they can burst open [72]. Bottom Left: Residual stress in plants can also be relieved by slicing them [76].

pith elongates and the outer tissues shorten by curving (See Fig. 14).

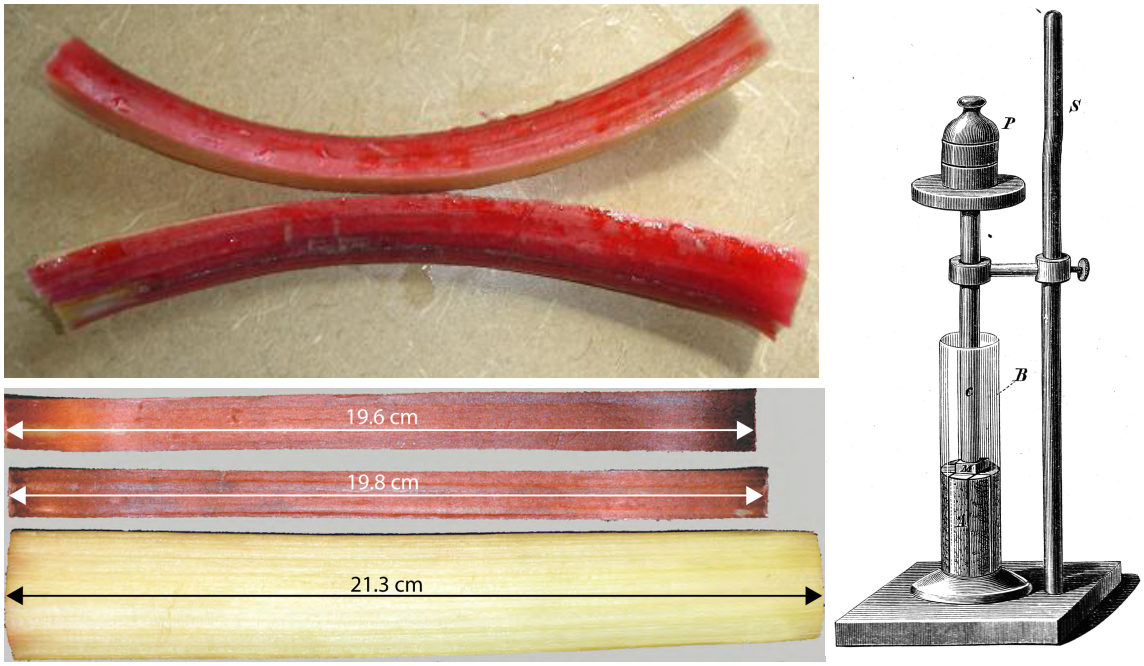

Figure 14: Residual stress in rhubarb. Top: A rhubarb would naturally curve backward when cut. Bottom: The middle segment of a long stalk of rhubarb was cut. This segment, of initial length 20 cm, was then peeled. The peeled strips are now shorter (by about 2-4%) and the pith is longer (by about 6%). The mutual tensions between inner and outer layers have been relieved. Left: The residual stress in the pith of the rhubarb can be measured by adding a weight to the top until its returns to its initial value [78].

The mutual tension between outer and inner tissues in rhubarb and its possible role in plant mechanics was mentioned as early as 1848 by Brucke, described by Sachs in 1857, and explored in detail by Hoffmeister in 1867 who noticed that the outer and inner tissues of *Vitis vinifera* (common grape vine) respectively, contract and extend elastically upon separation. The possible role of tissue tension in plant mechanics was well described by Sachs "*We have here the case of an elastic stiff body consisting of two parts, each in a high degree flexible and by no means stiff; only in their natural connection do the epidermal tissue and internal tissues together form an elastic rigid body*"[45, p. 216]. Following these early works, tissue tension became a central topic of interest in plant physiology as it was observed in many plants including wheat roots, fennel leaves, rhubarb stalks, sweetgum trees, and hypocotyls of cucumber, sunflower, cantaloupe, and squash. We attribute these stresses to the differential extension of the cell walls in outer and inner layers, creating an irreversible change in the resting lengths of both tissues [79].

Tissue tension also played a central role in the discovery of auxin as a growth hormone through the so-called "curvature pea-test" (See Fig. 15) [80]. As auxin acts differently on different tissues, the respective growth of the epidermis and pith of pea hypocotyl can be controlled by varying the auxin concentration and explicitly

tested by slicing the pea along its axis and measuring the resulting stem curvature. Despite the early success of mechanics in plant physiology, the advent of genetics and biochemistry changed the focus of plant development from a physical to a cellular emphasis. However, in recent years, the study of tissue tension (sometimes called *growth stresses* in trees [81]) has regained interest [82] and the role of tissue tension in growth regulation has become a controversial topic [73].

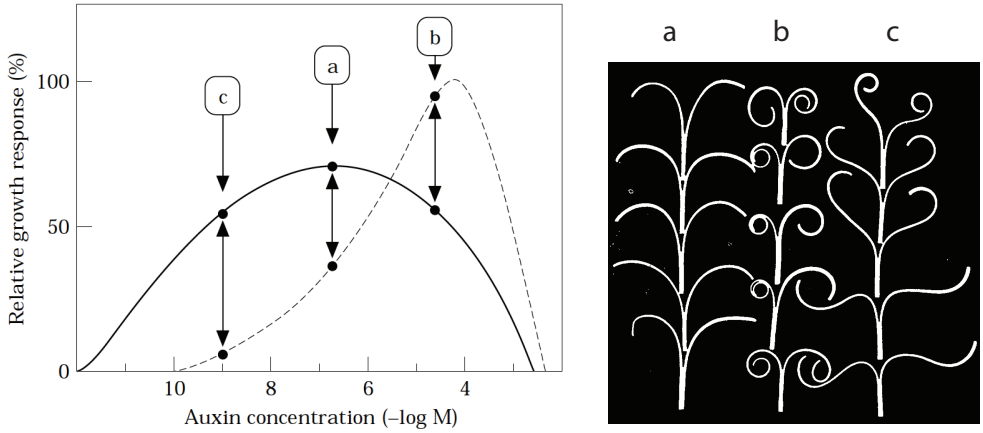

Figure 15: Pea test to determine the role of plant growth hormone [73], experiments with various level of auxin from Thiman and Schneider [83].

In physiology, it is through the work of both Fung and coworkers and the joint work of Vaishnav and Vossoughi in the 1980's [84], that the importance of residual stress became appreciated. The classic experiment of Fung [85] consists in slicing a disk of artery and realising that it will naturally open due to its residual stress field (See Fig. 16). If we view the artery as a three-layer cylinder, the opening of the disk reveals that when closed the inner layer (composed by the media-intima as shown in Fig. 10) is in compression whereas the other layer (the adventitia) is in tension. The opening angle in arteries has becomes a standard way of quantifying residual strains [86]. The stresses associated with the opening angle are known to play a fundamental role in regulating transmural stress gradient and lowering circumferential stress at the inner walls [87]. Experimental observations [88] also indicate that, not unlike the dandelion and the rhubarb, arteries also exhibit axial residual stress due to the relative axial growth of the different layers as first noted by Bergel [89] in the 1960's. However, the effect of axial residual stress and the axial pre-stretch in regular homeostasis still remains to be elucidated.

Once the importance of residual stresses in arteries was established, it was not long before residual stress was observed in a number of physiological systems (See Fig. 17) such as the oesophagus [90], the aorta [91], the heart [92], the trachea [93], the brain [94], bones [95], the developing embryo [96], as well as other systems such as solid tumours [97] and even in the drying of fruits [98] and in the aging of meat [99]. Residual stresses are a hallmark of living tissues and organs but play also an important role in many elastic systems as first noted by Ciley in 1901 [100] and manufactured systems [101] (see also the reviews [102] for an interesting discussion of the techniques used in engineering and bioengineering to measure residual stresses and their various

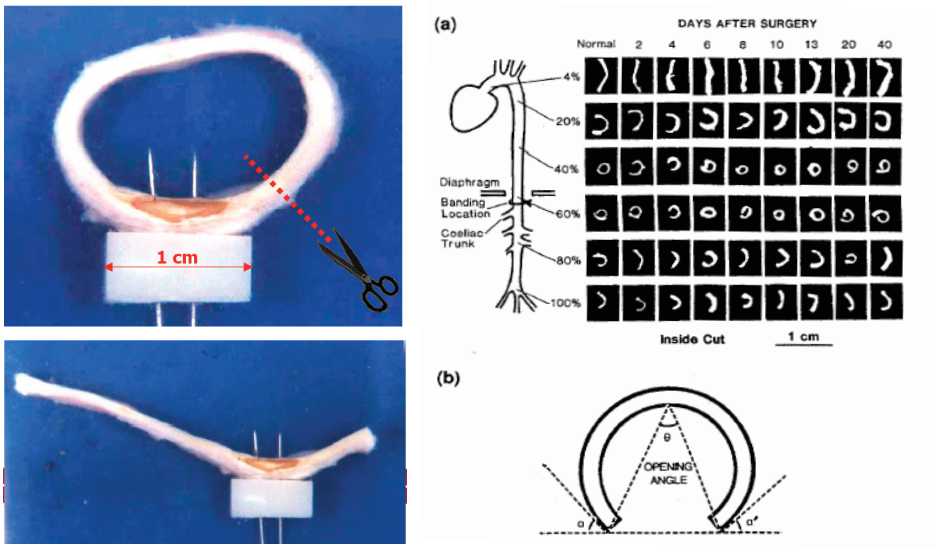

Figure 16: Residual stress in arteries. Left: Slicing a disk of artery typically shows that the artery opens relieving some of its residual stress (Picture from Holzapfel and Ogden). Right: Fung classic experiment and the definition of the opening angle.

effects on the properties and behaviours of different structures).

1.6 Basic questions in a theory of growth, the theory of morphoelasticity

From a geometric point of view, residual stresses arise due to the incompatibility between a specification of the local change in volume element and the continuity and integrity of the body. This is easy to visualise in a one-dimensional analogy of the rhubarb experiment. Consider a sandwich of three identical elastic rods perfectly glued to each other along their length and only allowed to deform along their length. Then, we let the middle rod increase uniformly in length. To preserve the integrity of the composite body, the middle rod must be compressed and the outer two rods must accordingly stretch. This structure has developed residual stress that could be relieved by two cuts (simply removing the glue between the layers would release all stresses) allowing the three rods to return to their original length. Interestingly, the shape of the grown composite body depends not only on the geometry but also on the elasticity of the three rods. Indeed, if the outer rods are very stiff, very little deformation will take place.

This elementary example outlines the interplay between the elasticity of the material, the local change in volume due to growth, and the overall geometry of the body. Further, stresses also influence growth through the evolution laws creating further dynamical coupling in the evolution of stresses and geometry. Understanding completely this coupling for given material and growth evolution laws in a given geometry is the central problem of a theory of *morphoelasticity*, that is a theory that couples growth evolution, geometry, and elastic response [104, 105]. The goal of such an approach is not only to obtain the new grown shape and the residual stress developed in the

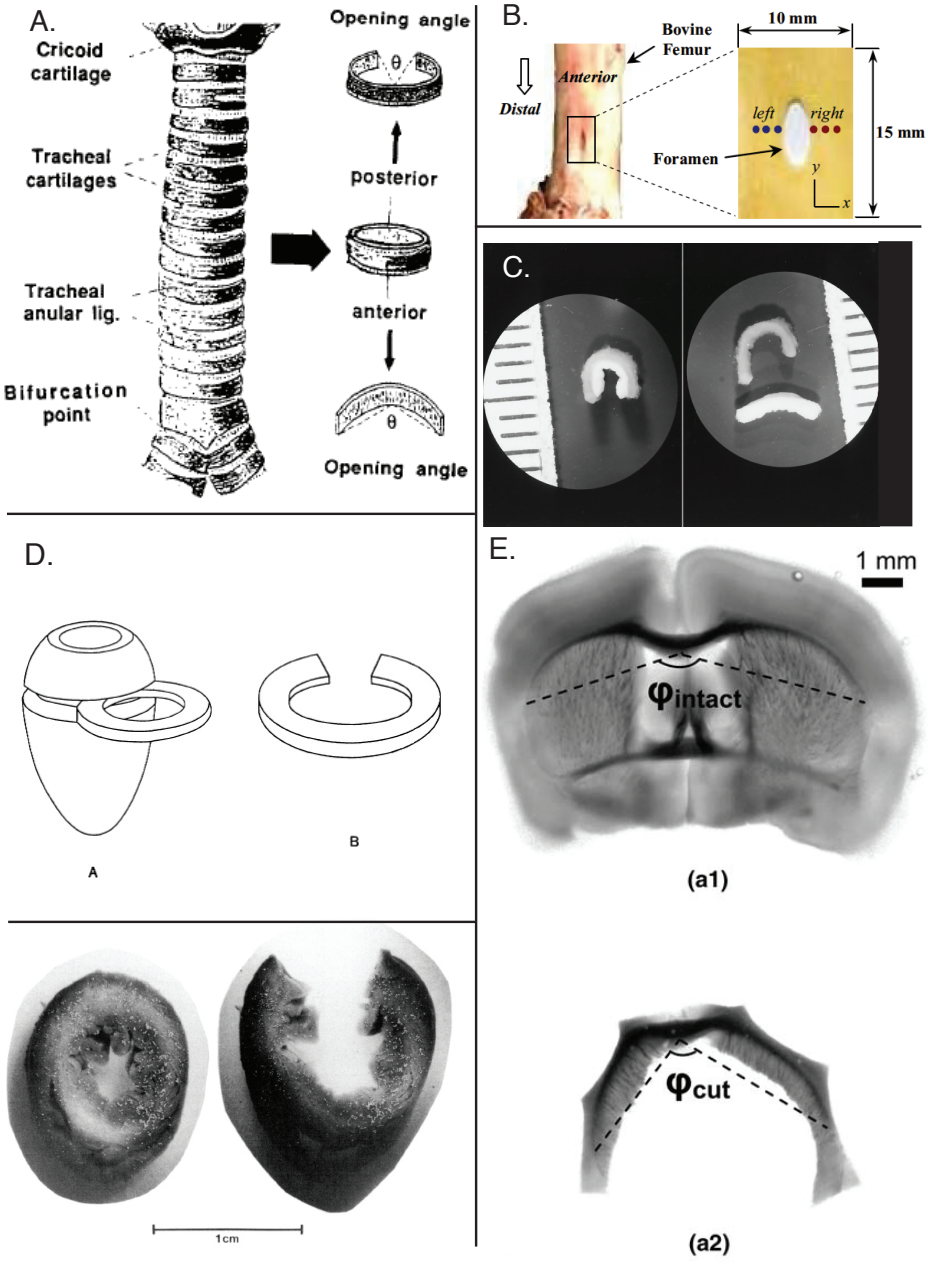

Figure 17: Evidence of residual stress in physiological systems. A. The trachea [93]. Notice how a cut in a disk relieves stress by opening. B: Bones [103]. Here an incision creates an opening due to tension C: The oesophapgus [90]. Different layers have different opening angles D: The heart [92]. A slice of heart also opens when cut. E: The brain [94].

structure but also to understand how such a new body evolves dynamically, how it responds to loading, and how it fulfils key structural and biological functions. For instance, it clearly appears that the grown rhubarb or dandelion is stiffer while grown and residually stressed than the different tissues it is made of at rest. Similarly, it is believed that arteries develop residual stress to regulate hoop stress that may cause tissue separation. How is this structure obtained dynamically? How does it evolve its material response during loading?

Yet another way that growth and elasticity can be combined in biological materials is through the formation of new morphological patterns born as mechanical instabilities [106]. Indeed, it is well-known that elastic materials under external loads can develop instabilities such as buckling [107] or wrinkling and a natural question is whether growth itself can generate sufficient stress as to destabilise the body. This is not obvious since the geometric effect of growth is to change the different length scales associated with the body (such as thickness) and this may also have a stabilising effect as, typically, stubby bodies are more stable than slender ones under compression. Therefore, geometric and mechanical effects can both help stabilise a structure for proper function [108] or destabilise the body to develop new shapes as found in 3D as well as in plates, shells, and membranes [109].

The general questions of interest in developing a mechanical theory of growth are in understanding the origin of the coupling between growth and mechanics as well as its consequence for biological functions or shapes:

- What is the role of mechanical cues in growing tissues?
- How does growth modify the structural properties of a tissue?
- What is the combined role of mechanics, geometry, and growth in morphological pattern formation?

2 One-dimensional growth

Overview

We consider the simplest possible growing system, a rod growing along a line. In this case, there is only one strain associated with the mechanics (the elastic stretch) and one strain associated with growth (the growth stretch).

To understand growth processes, it is instructive to start with simple, one-dimensional example: the growing rod. Rods are slender elastic structures that can support bending, twisting, stretching, and shearing. We first constrain growth on the line. When restricted to deformation in one-dimension, rods support only stretching and, in the case of growing rod, extension due to increase of mass. This filamentary structure

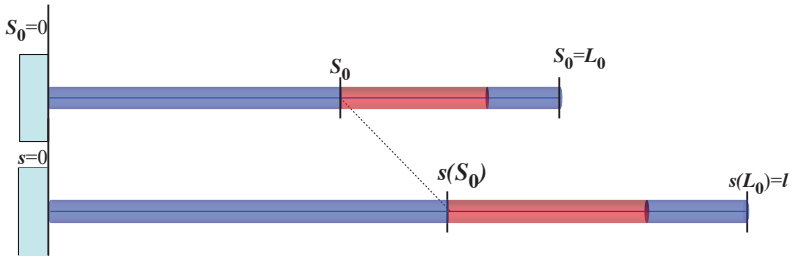

Figure 18: Extension of a filament in one-dimension. Initially of size L_0, the filament changes its length due to growth or stretching o a size l.

is parametrized by a parameter S_0 denoting the arc length of a material point from one end at time $t = 0$ (say, the left end, taken to be $S_0 = 0$) in an initial unstressed configuration (see Fig. 18). This rod is initially of length L_0. The rod can change its length and a point initially at a position S_0 is located in the current configuration at a position $s = s(S_0)$ and its total length in the deformed configuration is $s(L_0) = l$. The stretch variable denoting the local change of length is

$$\lambda = \frac{\partial s}{\partial S_0}. \tag{10}$$

If all segments of the rod experience the same stretch, the deformation is uniform and λ is simply given by $\lambda = l/L_0$. In general, at any point, $\lambda > 1$ implies that there is a local increase in length whereas $\lambda < 1$ represents a local decrease in length with respect to the initial configuration. A change in length can either be due to growth or applied loads, such as tension or compression. These are very different processes. To illustrate these differences we consider different growth mechanisms and loadings of the rod.

2.1 Pure elastic deformations

If the rod is put under a tensile stress σ (a *stress* is a force per area, specifically for a rod under uniaxial stress it is the force along the axis divided by the cross-sectional area), there is an elastic energy associated with the new configuration. This energy can be recovered by releasing the end and work can be provided. In such case, the

stretch is purely elastic, $\lambda = \alpha$, and the deformation is specified by a *constitutive law* that relates stresses to strains and provides information on the elastic nature of the material. For illustrative purpose, we start by assuming, a Hookean bahaviour, that is the simplest spring-like response proportional to the displacement and characterised by a single parameter, the Young modulus E. Then, we have

$$\sigma = E\epsilon = E(\alpha - 1). \tag{11}$$

where ϵ is the displacement associated with changes in length. If E is homogeneous (independent of the material and current position), this last relation completely specifies the deformation. For example, consider a beam deforming under its own weight. let the beam be originally of length L, have uniform density ρ, and cross-sectional area A.

Sagging under self-weight

We conclude that the current length is

$$l = L - \frac{\rho g L^2}{2EA} \tag{12}$$

The Hookean law (11) is only typically valid for small deformations. For large deformations, the theory of three-dimensional elasticity (developed later in this module) applied to the uniaxial extension of an incompressible rectangular *neo-Hookean* bar suggests the following nonlinear law

$$\sigma = \mu(\alpha^2 - \alpha^{-1}), \tag{13}$$

where μ is the *shear modulus*. Close to $\alpha = 1$, we recover the behaviour of the Hookean material (11) and we can identify $E = 3\mu$ (as shown in Fig. 19). More generally, materials that show strain-stiffening (increase in stiffness for large deformations) or strain-softening (decrease in stiffness) can be modeled by various function of the stretch, in which case the constitutive response in one dimension will be given by a general function

$$\sigma = f(\alpha), \tag{14}$$

with the requirement that $f(1) = 0$ and that the derivative of f at $\alpha = 1$ exists. For such systems, the Young modulus $E = f'(1)$ is then simply the linearized behavior for small deformations around the stress-free state.

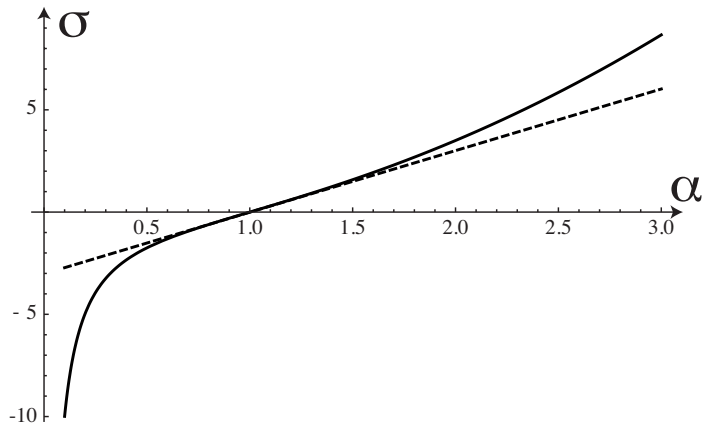

Figure 19: Comparison between the linear (dash) and nonlinear (solid) Hookean response for $\mu = 1, E = 3$.

2.2 Growth without elastic response.

If the rod has grown and there is no applied load, the rod also increases in length. This increase in length can be specified by a local growth stretch analogous to the elastic stretch. That is, we write $\lambda = \gamma$. The question is now to find a suitable description of the function γ which models a growth process taking place in time so that $\gamma = \gamma(t)$. It is easier and more natural to describe a growth process as a rate representing the changes occurring in a small increment in time. Therfore, we postulate the existence of an *evolution law* of the form

$$\frac{\partial \gamma}{\partial t} = G(\gamma, s, S_0). \tag{15}$$

For instance, uniform linear growth is achieved by taking $G = 1$ and, in the absence of other loads, we have at time t, $s = tS_0$ and the rod at time t has length $l(t) = (t+1)L_0$.

As a simple but important example, if the rod is made of cells that reproduce at a constant rate (as found, for instance, in the bacterial fibers of *Bacillus subtilis*, the rate of growth is proportional to the local growth stretch that is,

$$\frac{\partial \gamma}{\partial t} = k\gamma, \tag{16}$$

which results in exponential growth of the rod

$$s = S_0 e^{kt}, \quad l(t) = L_0 e^{kt}. \tag{17}$$

2.3 Application to spheroid tumor growth

2.3.1 Background

As an application of the idea of linear growth, we consider a simple model for tumor growth where a spherically shaped tumor expands its radius depending on the level of nutrient diffusing through its boundary. This model is part of a large class of experimental and theoretical models used in oncology referred to as *spheroid models*

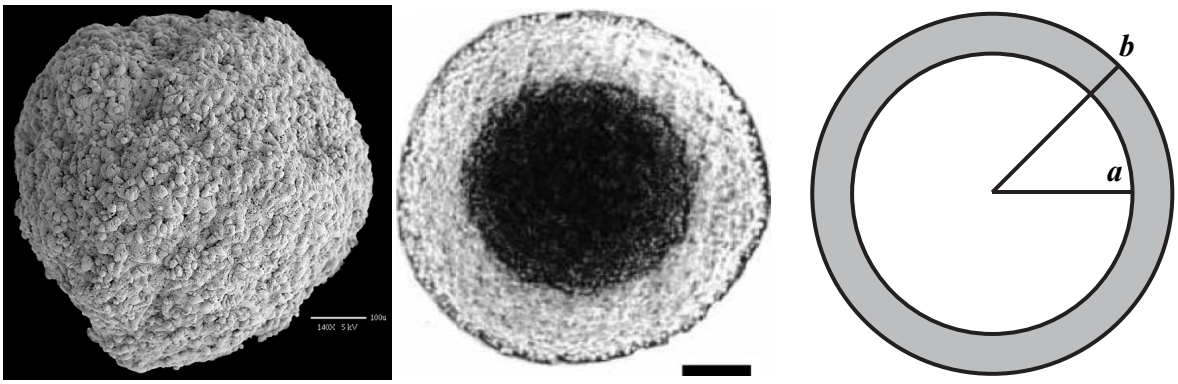

Figure 20: Multicellular tumour spheroids. Left: three-dimensional structure. Center: Cross section reproduced WITHOUT permission from [66]. The inner necrotic core is surrounded by a layer of quiescent cells. This layer is surrounded by a layer of active cellsÑthe bar is 250 mm. Right: Geometry of the problem

[110]. Experimentally, cancer cells can be cultured *in vitro* to grow on a gel or in a pool of nutrients and form a sphere-like shape, the spheroid [67, 111] (See Fig. 20). These spheroids are of great interest as they can be used in a variety of settings to understand the response of cancer cells under different physical, chemical, and genetic treatments [68, 70]. Mathematically, the spherical symmetry of these aggregates allows for a reduction of the problem difficulty by only considering the evolution of the radius [69].

2.3.2 The model

We model tumour spheroid as perfect sphere of radius $b(t)$ as a function of time t. Initially, the radial position of a material point inside the tumor is R_0 with radius B_0 and we are interested in the evolution of each point as a function of time, that is $r = r(R_0, t)$ and, in particular, the radius of the tumor $b(t)$.

Since, we assume radial symmetry, we can focus our attention on any line from the origin to the boundary of the sphere. We assume that growth is isotropic, that is, there is no preferred direction of growth, a volume element dV_0 initially located at a point R_0 will grow to a new volume element dv at the point $r = r(R_0, t)$ with a volumetric growth coefficient $\eta = \eta(r, R_0)$ which could depend on the type of cells (dependence on the original R_0) or its position r in the sphere.

Growth strain

That is,

$$\gamma = \eta R_0^2 r^{-2}. \tag{18}$$

In the absence of elastic response, the problem is equivalent to the growth of a rod. We assume that at each point, growth is exponential but proportional to the nutrient concentration $u(r,t)$, so that

$$\frac{\partial \eta}{\partial t} = k\eta u(r,t), \tag{19}$$

$$\frac{\partial r}{\partial R_0} = \gamma, \tag{20}$$

where $u(r,t)$ satisfies a diffusion equation

$$\frac{\partial u}{\partial t} = \frac{D}{r^2}\frac{\partial}{\partial r}\left(\frac{r^2 \partial u}{\partial r}\right) - Q. \tag{21}$$

Here D is the diffusion constant and Q is a constant nutrient uptake. The tumor is assumed to sit in a well-mixed bath of nutrients so that the concentration at the outer surface is $u(b,t) = u_b$.

2.3.3 Analysis

Starting with a small size tumor, we expect the nutrient to penetrate all the way to the origin. However, as the tumor grows, it will reach a critical size b_{cr} at time t_{cr} so that the concentration at the origin vanishes $u(0, t_{cr}) = 0$. Since the concentration remains positive for all time, for $t > t_{cr}$, the concentration will vanish at a point a with $0 < a < b$ (see Fig. 21).

Concentration profile

That is,

$$u(r) = \frac{Q}{6D}(r^2 - b^2) + u_b \tag{22}$$

if $b < b_{cr}$ and

$$u(r) = \begin{cases} 0, & r < a, \\ \frac{Q}{6D}r^2 + \frac{Q(b^3-a^3)-6Dbu_b}{6(a-b)D} + \frac{abQ(a^2b^2)+6abDu_b}{6(a-b)D}\frac{1}{r} & r > a. \end{cases} \tag{23}$$

if $b > b_{cr}$

The critical radius b_{cr} is found as the first radius for which $u(0) = 0$ which leads to

$$b_{\text{cr}} = \sqrt{\frac{6Du_b}{Q}}. \tag{24}$$

For $b \geq b_{\text{cr}}$, the inner radius a is determined by the condition $\frac{\partial u}{\partial r}|_{r=a} = 0$, that is the first positive root of the polynomial

$$P(a, b) = Q(2a^3 - 3a^2b + b^3) - 6bDu_b. \tag{25}$$

In Fig 21, the nutrient profile is shown for different values of the external radius. The inner shell of radius a can be associated with the so-called *necrotic core*[3], a region inside the spheroid where the cells die due to lack of nutrient. As the radius increases,

[3]We comment again on the fact that this is an over-simplified view of the problem as a quiescent zone can also formed where the cells do not proliferate but remain alive and are in a state of dormancy [112, 113]. Nevertheless, this toy model captures the essence of the problem and give a basis for the concepts of penetration length, proliferating zone, and necrotic core frequently used in the study of tumor growth [114].

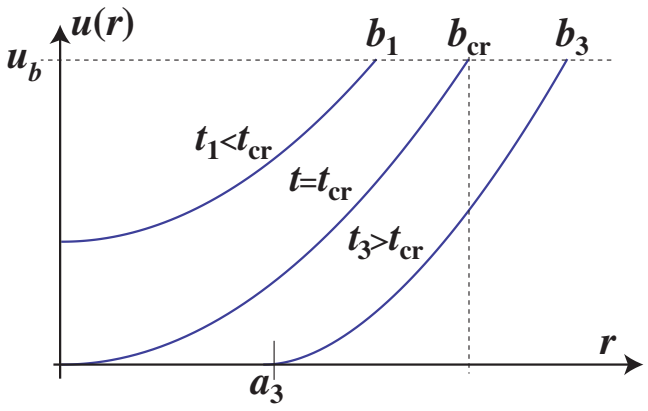

Figure 21: Nutrient profile as a function of the radius. For $t < t_{cr}$, the nutrient penetrates in the spheroid to the origin. For $t = t_{cr}$, the profile vanishes at the origin and for $t > t_{cr}$, a necrotic core.

the proliferating zone $(b - a)$ tends rapidly to a constant determined by the solution of (25) for large b, that is

$$\Delta = \lim_{b\to\infty}(b - a) = \sqrt{\frac{2Du_b}{Q}}. \tag{26}$$

Once the nutrient profile is known, the growth of the tumor can be computed by integrating (19).

Growth profile

That is, the equation for the outer radius is

$$\frac{\partial b(t)}{\partial t} = kb^{-2}\int_0^b u(\rho, t)\rho^2 d\rho. \tag{27}$$

Initially, the entire spheroid is proliferating and we observe exponential growth (see Fig 22). As the necrotic core forms, growth is still exponential but in a region of constant width. Therefore, following the argument in the previous section on tip growth, we conclude that, for large b, the radius should increase linearly in time as shown in Fig. 22.

2.3.4 Discussion

Apart from the effect of nutrient, it is believed that mechanical stress has also an effect on growth as high stress may limit the ability of cells to divide through contact inhibition[70, 115]. However, in order to investigate the effect of mechanics on growth, an analysis of the full stress tensor at any point in the spheroid needs to be performed.

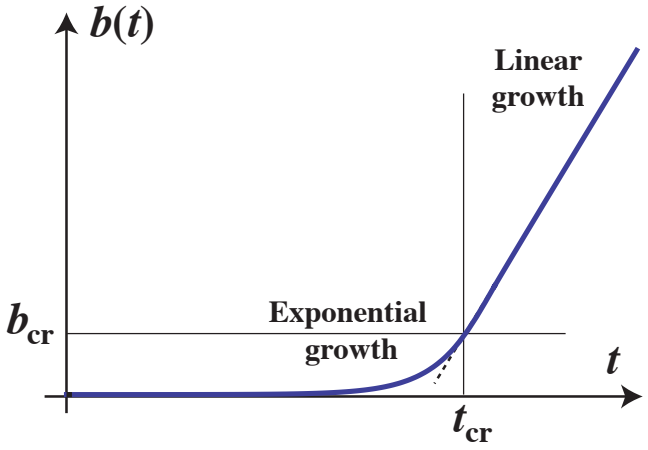

Figure 22: Left: Nutrient profile as a function of the radius. For $t < t_{cr}$, the nutrient penetrates in the spheroid to the origin. For $t = t_{cr}$, the profile vanishes at the origin and for $t > t_{cr}$, a necrotic core. Right: Evolution of the radius as a function of time. For short time, the tumor grows exponentially, for $t > t_{cr}$, a necrotic cored develops and only a spherical shell proliferates.

2.4 Growth with elastic response

So far, we have considered growth and elastic deformations as two independent processes involved in changing locally the length of a filament. In general, growth may induce stresses. For instance, if we let a filament grow between two rigid plates, the ends cannot move as the rod grows and compressive stresses are generated. By contrast, growth may be triggered or influenced by stresses in the material. Therefore, growth and elasticity may be coupled and and we must integrate them within a single framework. The fundamental assumption of *morphoelasticity* is that the change in length is due to both processes so that we can write

$$\lambda = \alpha\gamma. \tag{28}$$

This apparently simple multiplicative decomposition is rather subtle and needs to be further discussed and justified in the general context of nonlinear elasticity. Before discussing this problem in more detail, it is of interest to explore the consequences of such a decomposition by considering different situations.

2.4.1 Growth of a rod constrained between two plates

First, we consider a growing rod between two plates. That is, we allow no displacement of the ends. If the rod grows uniformly and linearly in time (that is, $\gamma = 1 + t$), it creates a uniform compressive stress. Therefore, we have $\lambda = \alpha\gamma = 1$ and $\alpha = 1/(t+1)$ which implies, if we assume again a constitutive relationship (11),

$$\sigma = -\frac{Et}{t+1} \tag{29}$$

and, paradoxically, it appears that the stress saturates asymptotically to $-E$ as $t \to \infty$. This is due to the fact that, within the assumption of the Hookean law (11), it takes a finite stress (namely $-E$) to compress a rod to zero length. Clearly, real materials will not follow this behavior and corrections to the Hookean law will enter the constitutive relation when compression (or tension) becomes sufficiently large. For instance, using the neo-Hookean law (13), we obtain

$$\sigma = \mu\left(\frac{1}{1+t^2} - t + 1\right), \tag{30}$$

and an infinite compressive force ($\sigma \to -\infty$) is generated as the bar elongates indefinitely as $t \to \infty$.

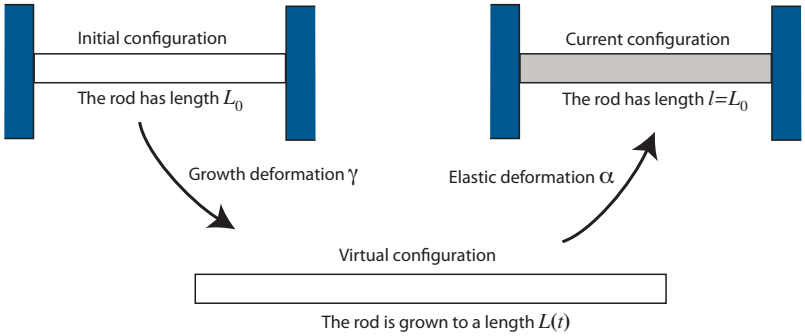

Figure 23: The growth of a constrained rod between two plates can be thought of as the composition of two distinct processes: a growth deformation which creates a stress-free virtual configuration, followed by an elastic deformation necessary to enforce the boundary conditions.

A slightly different way to understand the coupling between growth and elasticity is to separate the response of the material into two distinct processes. First, we apply the growth deformation, that is we let the rod grow without the external constraints of the plates, so that at any given time, it is in an unstressed state but grown in such a way that the material point S_0 is now at a position $S(S_0, t) = S_0(1 + t)$ with total length $L(t) = L_0(1+t)$. Since, this state is not realized in the experiment in question, we refer to it as a *virtual configuration*, that is, a useful mathematical construct needed to find a solution of the problem. Second, we place the grown configuration back in between the plates, that is we find the elastic stretch $\alpha = 1/(t + 1)$ necessary to compress the rod.

This example also provides a simple illustration of one of the fundamental problems related to the modeling of growth, that is the *evolution of the reference configuration*. In order to evaluate the elastic deformation and the stresses in a growing material, one needs to define the strain which is a measure of the deformation with respect to a reference configuration which is a configuration where the material is unstressed. As growth takes place, the reference configuration of the material evolves. For instance, in our example, the reference configuration is not the initial configuration but the virtual configuration obtained by removing stresses, that is, $\alpha = 1$, which corresponds to a filament of length $L = L_0(t + 1)$. In this book, we will use the following notation: lowercase denotes a variable in the current configuration, whereas uppercase designates the similar variable in the unloaded configuration either initially (with subscript 0) or at any given time (without subscript or with a subscript t is necessary).

The standard picture of elasticity is to consider an initial reference configuration without stresses and a current configuration where loads are applied and stresses can be computed from the mechanical balance and constitutive equations. We see on this simple example that an understanding of the stresses in a growing elastic medium requires yet another configuration, namely the virtual configuration, where the material has grown but in which there is no stress. In the case of one dimensional extension, the experiment of removing the stresses by unloading the material can always be carried out. However, we will see that in many situations this configuration cannot be achieved by a physical experiment but can only be defined locally, hence the name *virtual configuration*, a mathematically useful, but often physically unattainable construct.

2.4.2 Stress dependent growth.

We now consider a situation where growth and stresses are coupled. We assume that the filament has a natural *homeostatic stress* σ^*, that is, a stress that the filament, through the active process of growth, tends to recover when disturbed out of its natural state. Here, for illustrative purpose, we assume that this process can be modeled by the evolution law

$$\frac{\partial \gamma}{\partial t} = \gamma(\sigma - \sigma^*), \tag{31}$$

which implies that exponential growth (or resorption[4]) will take place until the stress σ reaches the homeostatic stress σ_*.

Assuming again a Hookean stress-strain relationship $\sigma = E(\alpha - 1)$, we see that there is a unique homeostatic strain $\alpha^* = 1 + \sigma^*/E$. We now consider the following problem: we assume that at time $t = 0$, the filament is happily resting in a state of homeostatic stress with a length l_0. The filament is instantaneously extended to a constant length l. How will the filament evolve to reestablish its homeostatic stress?

[4]Again, growth is understood as either an increase (positive growth or densification) or decrease (negative growth or resorption) of mass or volume.

Growth with stress

That is,

$$\gamma(t) = \frac{l}{l_0} + \left(1 - \frac{l}{l_0}\right) e^{-(E+\sigma^*)t}. \tag{32}$$

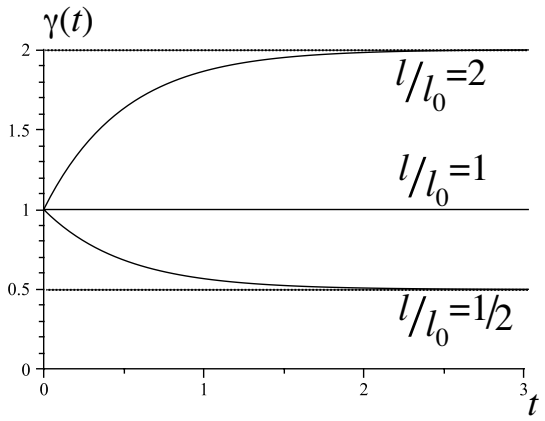

Figure 24: Growth evolution of a filament with homeostatic stress σ^* of length l_0 either extended to a filament of length $l = 2l_0$ or compress to a filament of length $l = l_0/2$ ($\sigma^* = 1$).

As expected the filament grows as to recover its homeostatic stress σ^*. The notion of homeostatic stress is central in understanding normal maintenance and function of many tissue (*homeostasis*).

3 A growing rod

■ Overview

We can generalise the ideas of growth to the case where the rod can evolve in space while growing axially.

3.1 Kinematics of a growing rod

Based on the general approach of growth in nonlinear elasticity through a multiplicative decomposition [116, 106], we consider three different configurations for the rod. The *initial configuration* $\mathcal{B}_0$ is the unstressed configuration of the rod at time $t = 0$, all quantities in this state are denoted by a subscript 0. The *reference configuration* $\mathcal{V}$ is the unstressed configuration at a given time t and the *current configuration* $\mathcal{B}$ of the rod is the actual configuration of the rod at time t for given external loads, body loads and boundary conditions. Note that at time t the unstressed configuration may not be realizable in the Euclidian space. For instance, starting initially with a ring of radius one and unstressed curvature one and increasing the rod length while keeping the unstressed curvature constant would lead to a stress-free configuration that would be self-penetrating. However, unlike the three-dimensional case, there is no problem with local compatibility and generation of residual stress associated with the local definition of a growth and elastic tensor [105]. Therefore, all local quantities are well-defined and the reference configuration is appropriate for the computation of the current configuration.

At time $t = 0$, the rod is described by its unstressed shape $\hat{\mathbf{u}}_0 = \hat{\mathbf{u}}(S_0, t = 0)$ with arc length S_0, total length L_0, density $\rho_0(S_0)$, cross-sectional surface area $A_0(S_0)$ and a stiffness matrix $\mathbf{K}_0$. This unstressed shape evolves so that at any given time t the rod has unstressed shape $\hat{\mathbf{u}} = \hat{\mathbf{u}}(S_0, t)$, with arc length S, total length $L(t)$, density $\rho(S_0, t)$, cross-sectional surface area $A(S_0, t)$ and a stiffness matrix $\mathbf{K}$. In this description, S_0 is now a material parameter. It is related to arc length S of the virtual configuration $\mathcal{V}$ by the *growth stretch* γ, i.e.

$$\gamma(S_0, t) = \frac{\partial S}{\partial S_0}, \tag{33}$$

so that γ characterizes the local increase of length of a material segment located at a material point S_0 at time t. This virtual configuration is required in order to compute the current shape of the rod for given loads and boundary conditions (See Figure 25). In the current configuration, the rod has arclength s and total length $l(t)$.

3.2 Mechanics

We define α to be the *elastic stretch* and λ the *total stretch* between the initial and current configuration, so that the decomposition of growth follows from the simple chain rule

$$\lambda = \alpha\gamma \quad \Longleftrightarrow \quad \frac{\partial s}{\partial S_0} = \frac{\partial s}{\partial S}\frac{\partial S}{\partial S_0}. \tag{34}$$

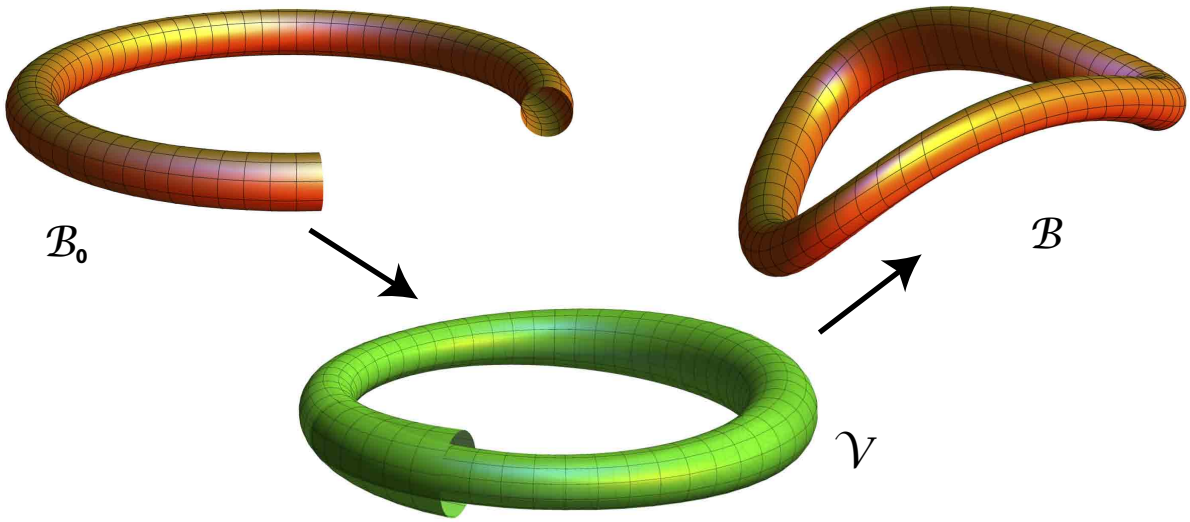

Figure 25: Schematic of the 3 configurations, initial $\mathcal{B}_0$, reference $\mathcal{V}$, and current $\mathcal{B}$. The reference configuration is stress-free and evolves in time and reflects the change due to growth (shown here, initially the rod has intrinsic curvature; as growth proceeds the cross-section is allowed to grow inhomogeneously and the length of the rod increases). The reference configuration can also intersect itself as it does not represent a possible realization of the rod; rather, it defines its local properties. The current configuration is the actual configuration with correct boundary conditions (here periodic boundary conditions) and body loads.

At time t, the balance of force and moment in the reference configuration yields

$$\frac{\partial \mathbf{n}}{\partial S} + \mathbf{f} = 0, \tag{35}$$

$$\frac{\partial \mathbf{m}}{\partial S} + \frac{\partial \mathbf{r}}{\partial S} \times \mathbf{n} + \mathbf{l} = 0, \tag{36}$$

where $\mathbf{f}$ and $\mathbf{l}$ are the body force and couple per unit *reference* length. The reference arc length S is the natural choice to express all quantities as the constitutive equations are given in the reference configuration. Explicitly, the resultant moments are

$$\mathbf{m} = EI_1(\mathsf{u}_1 - \hat{\mathsf{u}}_1)\mathbf{d}_1 + EI_2(\mathsf{u}_2 - \hat{\mathsf{u}}_2)\mathbf{d}_2 + \mu J(\mathsf{u}_3 - \hat{\mathsf{u}}_3)\mathbf{d}_3 \tag{37}$$

where E is the Young's modulus, μ is the shear modulus, J is a parameter that depends on the cross-section shape and and I_1 and I_2 are the second moments of area. In this case, in addition to (37), we have an equation relating the elastic stretch $\alpha \equiv \mathsf{v}_3 \equiv \frac{\partial s}{\partial S}$ to the tension

$$\mathsf{n}_3 = EA(\alpha - 1). \tag{38}$$

Note that the Darboux vector $\mathbf{u}$ is defined in the reference configuration, so that

$$\mathbf{u} = \alpha(\kappa \sin\varphi, \kappa\cos\varphi, \tau + \frac{1}{\alpha}\frac{\partial\varphi}{\partial S}) \tag{39}$$

where κ and τ are the usual *Frenet curvature and torsion*. For a straight rod under uniaxial tension, the constitutive equation (38) is simply Hooke's law. Note that although the Darboux vector $\mathbf{u}$ is scaled by a factor α in (39), the unstressed Darboux vector $\hat{\mathbf{u}}$ is given by the unstressed geometric curvatures in the reference configuration (it is not scaled by α since it is a material property of the rod in the reference configuration).

A change of independent variable leads to an alternative formulation in the current and initial configuration. Namely, we have

$$\frac{\partial \mathbf{n}}{\partial s} + \alpha^{-1}\mathbf{f} = 0, \tag{40}$$

$$\frac{\partial \mathbf{m}}{\partial s} + \frac{\partial \mathbf{r}}{\partial s} \times \mathbf{n} + \alpha^{-1}\mathbf{l} = 0, \tag{41}$$

where $\alpha^{-1}\mathbf{f}$ and $\alpha^{-1}\mathbf{l}$ are now the body force and couple per unit *current* length. Finally, in the initial configuration, we have

$$\frac{\partial \mathbf{n}}{\partial S_0} + \gamma\mathbf{f} = 0, \tag{42}$$

$$\frac{\partial \mathbf{m}}{\partial S_0} + \frac{\partial \mathbf{r}}{\partial S_0} \times \mathbf{n} + \gamma\mathbf{l} = 0, \tag{43}$$

where $\gamma\mathbf{f}$ and $\gamma\mathbf{l}$ are the body force and couple per unit *initial* length.

3.3 Remodelling

By remodelling we refer to a change in material parameters without a change in mass. For instance, we might consider a change in the rod's intrinsic curvature. An interesting phenomenon that can be well-modelled with this approach is gravitropism – see Fig 26. In gravitropism, a plant reorients itself to align with a gravitational field. This involves a complicated process that links activities at the cell level to tissue-level differential growth (cells on one side of the plant grow more than those on the other side). However, when viewed at the organ level, i.e. treating the plant or stem as an elastic rod, the length may not change, and we can understand the kinematics of this process as a remodelling of intrinsic curvature in response to gravity.

We describe the plant stem as a planar inextensible elastic rod given by $\mathbf{r}(s,t) = x(s,t)\mathbf{e}_x + y(s,t)\mathbf{e}_y$, and suppose that gravity is in the negative y-direction. Defining $\phi(s,t)$ as the angle between the tangent and the vertical, we have $\mathbf{d}_3 = \sin\phi\mathbf{e}_x + \cos\phi\mathbf{e}_y$, $\mathbf{d}_1 = \cos\phi\mathbf{e}_x - \sin\phi\mathbf{e}_y$. The rod only bends about the $\mathbf{d}_2 = -\mathbf{e}_z$, and the curvature vector is $\mathbf{u} = \mathsf{u}_2\mathbf{d}_2$ with $\mathsf{u}_2 = \partial\phi/\partial s$. Suppose further that the plant is clamped at one end ($s = 0$) at the origin and with fixed angle $\phi = \phi_0$.

The idea is that the intrinsic curvature changes locally (at each point along the stem) in response to how well-aligned the current tangent direction is with $\mathbf{e}_y$. A classic model for this is the 'sine-law', which states

$$\frac{\partial \hat{\mathsf{u}}_2}{\partial t} = -\beta \sin\phi \tag{44}$$

where β is a constant parameter characterising the rate of the response. Neglecting the deformation due to gravity, the curvature is exactly given by the intrinsic curvature,

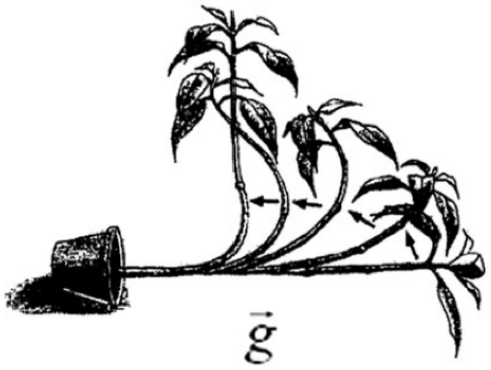

Figure 26: In gravitropism a plant oriented horizontally develops curvature to align with gravity.

i.e. $\mathsf{u}_2 = \hat{\mathsf{u}}_2$, and thus the kinematics is described by

$$\frac{\partial \phi}{\partial s} = \mathsf{u}_2 \tag{45}$$

$$\frac{\partial \mathsf{u}_2}{\partial t} = -\beta \sin \phi \tag{46}$$

Given $\phi(s,t)$, the shape of the stem can be determined from the geometry. If ϕ_0 is small, so that the plant is close to vertical, as asymptotic solution can be attained.

Gravitropism in nearly vertical limit

That is,

$$x(s,t) = \frac{\phi_0 s J_1(2\sqrt{\beta s t})}{\sqrt{\beta s t}} \tag{47}$$

where J_1 is the Bessel function of the first kind.

3.4 Mechanical pattern formation

One of the primary ways that biological systems "use" mechanics is to generate patterns. The idea is simple: mechanical forces that appear in a growing system can generate stresses that take the system from a 'trivial' base state to a 'complex' patterned state. For example, in a growing embryo, a hand begins as a uniform nearly spherical body; it is through differential growth and mechanical forces that a bifurcation occurs which eventually leads to the formation of fingers. This basic notion at some level underlies nearly all the structural patterns we observe, from the cortical folds in the brain to the shape of leaves to the fractal edge of lettuce, and many more. Here, it is important to distinguish between a biochemical pattern, i.e. a Turing pattern (which you may have studied in a previous mathematical biology course), in which chemical concentrations go from a homogeneous to a patterned state through reaction and diffusion. Here we refer to a *biomechanical* pattern, a structural pattern defined by the deformation of a material to a structural pattern. Though in practice, the patterns we see often will involve a combination of biochemical and biomechanical effects!

3.4.1 Rod on a foundation

A good model system for investigating structural pattern formation is a growing rod on a foundation. We consider the buckling of a planar rod on a substrate, or 'foundation'. The idea is that the rod models a growing tissue, but it is constrained by attachment to an underlying tissue; this constraint generates stresses in the system which are eventually relieved by a buckling pattern. This scenario is very common in the literature, and forms the basic idea underlying the morphogenesis of many patterns: e.g. wrinkles in the skin, ridges and spines in seashells, and the wavy epithelial pattern in airways and intestine. It is instructive to proceed in detail and see how the buckling pattern emerges from our morphoelastic rods framework. The rod is naturally straight, initially

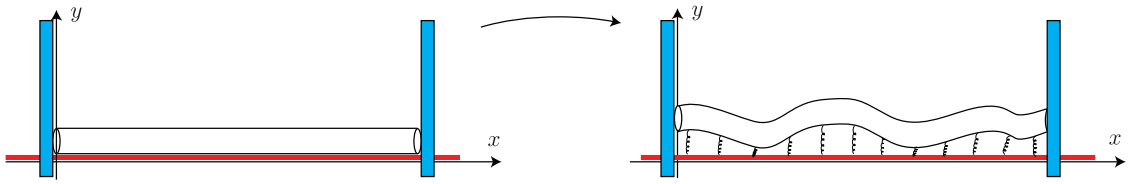

Figure 27: Setup of the buckling of a straight planar rod on a foundation. A rod is attached to a foundation and is allowed to deform only in the plane. An increase in length leads to a buckling instability.

planar and constrained in the plane so that with respect to the reference configuration $\mathcal{V}$ the Darboux vector is $\mathbf{u} = (0, \alpha\kappa, 0)$, where κ is the Frenet curvature. A convenient representation of the rod is obtained by assuming that it lies in the x-y plane and

introducing the angle θ between the tangent vector and the x-axis. That is

$$\boldsymbol{\tau} = \mathbf{d}_3 = \cos\theta \mathbf{e}_x + \sin\theta \mathbf{e}_y, \tag{48}$$

which implies

$$\kappa = \frac{\partial \theta}{\partial s} = \alpha^{-1} \frac{\partial \theta}{\partial S} \tag{49}$$

and $\mathbf{d}_2 = \mathbf{e}_z$. By writing $\mathbf{n} = F\mathbf{e}_x + G\mathbf{e}_y$, $\mathbf{f} = f\mathbf{e}_x + g\mathbf{e}_y$, $\mathbf{r} = x\mathbf{e}_x + y\mathbf{e}_y$, we can simplify the equilibrium equations (35-36) to a system of 5 equations in the current configuration

$$\frac{\partial x}{\partial S} = \alpha \cos\theta, \qquad \frac{\partial y}{\partial S} = \alpha \sin\theta, \tag{50}$$

$$\frac{\partial F}{\partial S} + f = 0, \qquad \frac{\partial G}{\partial S} + g = 0, \tag{51}$$

$$EI \frac{\partial^2 \theta}{\partial S^2} + \alpha G \cos\theta - \alpha F \sin\theta = 0. \tag{52}$$

These equations are supplemented by the constitutive law for the foundation (see below) and a constitutive law for tension $F\cos\theta + G\sin\theta = EA(\alpha - 1)$ where A is the cross sectional area as before. We use this last relationship to express α in terms of F, G and θ in the equations above.

We consider the case of a clamped uniformly growing rod of initial length $L_0 = 1$ and whose end positions are fixed for all time, that is

$$x(0) = 0,\ x(L) = 1,\ y(L) = y(0) = y_0,\ \theta(0) = \theta(L) = 0. \tag{53}$$

where y_0 is the distance between the rod and the rigid foundation taken to be the segment of the x-axis between 0 and 1. Different assumptions on the nature of the attachment between the rod and the foundation can be made. We consider here the case where the rod is initially glued to the axis. Therefore, a point $(S_0, 0)$ on the x-axis is attached to a point (S_0, y_0) on the rod. In the current configuration the two points are still connected elastically and are now located at $(S/\gamma, 0)$ and $(x(S), y(S))$. Therefore, the body force acting on the rod from the foundation is

$$\mathbf{f} = \frac{h(\Delta)}{\gamma\Delta} \left[(x - S/\gamma)\mathbf{e}_x + (y - y_0)\mathbf{e}_y \right] \tag{54}$$

where the rest length of the foundation is y_0 and $\Delta = \sqrt{(x - S/\gamma)^2 + (y - y_0)^2}$ is the distance in the current configuration between two material points connected in the initial configuration. Note the factor $1/\gamma$ which indicates that the attachment was made in the initial configuration and no subsequent remodeling takes place. The function $h(\Delta)$ is chosen such that $h(0) = 0$ and $h'(0) = -Ek < 0$.

A bifurcation analysis (see Problems) shows that there is a critical value of γ at which the solution (on an infinite domain) becomes unstable. In a finite domain, the amplitude of this periodic solution is modulated as shown in Fig. 28.

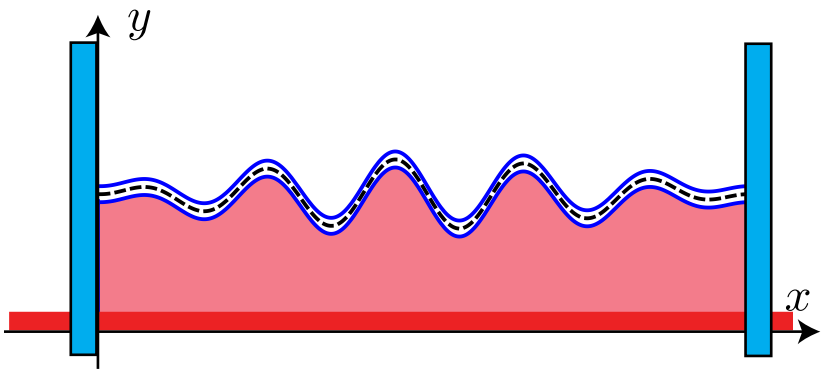

Figure 28: Buckling of a clamped growing rod on an elastic foundation. The rod is constrained to lie in the unit interval $L_0 = 1$ and is clamped at the boundary (with $y_0 = 1/2$). Here $k = 1, r = 0.02$, and $\gamma_2 = 1.19934$. The amplitude is arbitrary and chosen here to be $C_1 = -0.2$ and the centreline is indicated by a dashed line.

4 A brief review of classical nonlinear elasticity

■ Overview

Before incorporating growth in a general mechanical theory, it is worthwhile recalling the basic equations that describe the response of a continuum material under loads. This is a very brief review of classical nonlinear elasticity based on the lecture notes of Solid Mechanics.

When dealing with tissues and organs, it is now well appreciated that many such systems operate in large deformations. For instance, large arteries are typically stretched between 20% to 60% from their unloaded configurations [117]. It is also known from the work of biomechanicians that the nonlinear response of soft-tissues differs qualitatively from the response of elastomers (rubbers). A striking example is shown in experiments first performed in the 19th Century [118]. A cylindrical or spherical elastic membranes is pressurised (See Fig. 29). At a critical pressure, an elastomer will suddenly jump to a new spherical equilibrium whereas a soft-tissue (here a dog bladder) will reach an asymptotic radius. This difference in behaviour is due to the composition of many soft-tissues. Typically, soft-tissues are a blend of an elastic matrix reinforced by fibres (elastin and collagen respectively in the case of animal tissues) and the limiting behaviour is obtained when the stiff fibres are fully extended and resist further deformations. Further, biological materials are highly inhomogeneous and typically anisotropic (again due to the particular orientation of the reinforcing fibres). Therefore, a continuum theory for the mechanical response of biological tissue requires the general theory of nonlinear elasticity, which, by contrast to the theory of linear elasticity neither assumes small deformations, a particular choice of constitutive law, nor a particular symmetry of the material (note however, that we will mostly be concerned here with the case of isotropic response). It is also the natural framework to develop a theory of growth and remodelling.

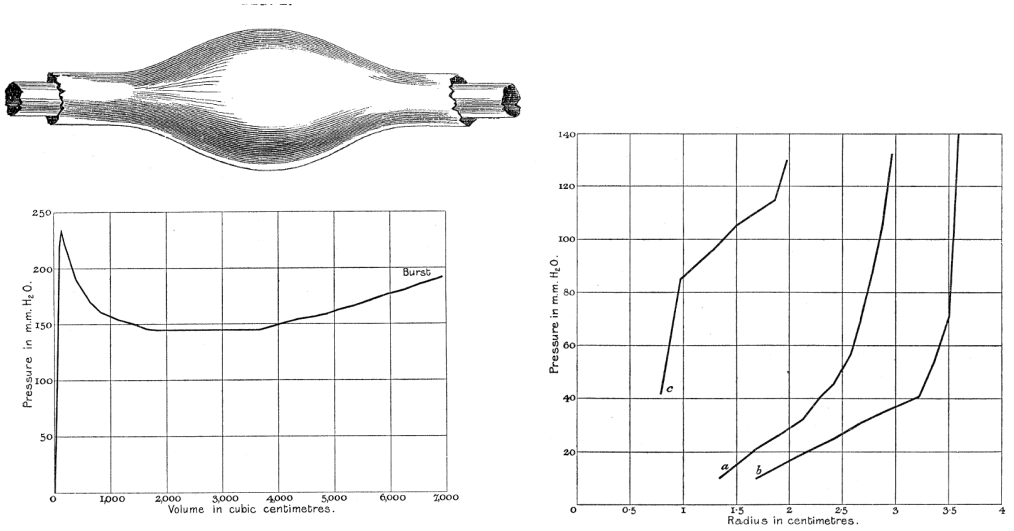

Figure 29: The important of nonlinearities and large deformations is demonstrated in a pressure experiment as originally investigated by Mallock in 1890 [118] (top picture). The experiment consists in increasing the pressure inside a tube or a sphere while recording the radius of the bulge. In the case of rubber (Left), a sudden limit-point instability is observed at a critical pressure in an experiment by Osborne and Sutherland [119]. The radius past that critical pressure will suddenly increase. However, in the case of a biological tissue, the behaviour is qualitatively different and the instability disappears (Right). In that case it will be increasingly harder to increase the size of the bulge by increasing the pressure.

4.1 Kinematics

In nonlinear elasticity one considers two configurations for the description of a body. A *body*, B is a set whose elements can be put into 1-1 correspondence with points in a region $\mathcal{B} \subset \mathbb{E}^3$. Since the body moves or deforms, it can change with time $t \in \mathbb{R}$. We denote by $\mathcal{B}_t$ the *configuration* of B at time t. In particular if we look at static systems, we will use $\mathcal{B}_0$ for the *initial configuration* and $\mathcal{B}$ for the *current configuration*. The initial configuration $\mathcal{B}_0$ is parameterised by points relative to the position vector $\mathbf{X}_0$ and the current configuration by the position vector $\mathbf{x}$. Since the body retains its integrity and material points do not overlap, both $\mathcal{B}_0$, $\mathcal{B}_t$ are bijections of B. Therefore there exists an invertible mapping, called *deformation* or *motion* $\boldsymbol{\chi} : \mathcal{B}_0 \to \mathcal{B}_t$ such that

$$\mathbf{x} = \boldsymbol{\chi}(\mathbf{X}_0, t), \quad \forall\, \mathbf{X}_0 \in \mathcal{B}_0 \qquad \text{and} \qquad \mathbf{X}_0 = \boldsymbol{\chi}^{-1}(\mathbf{x}, t), \quad \forall\, \mathbf{x} \in \mathcal{B}_t. \tag{55}$$

This mapping is pictured in Fig. 30. It is convenient to use two orthonormal Cartesian

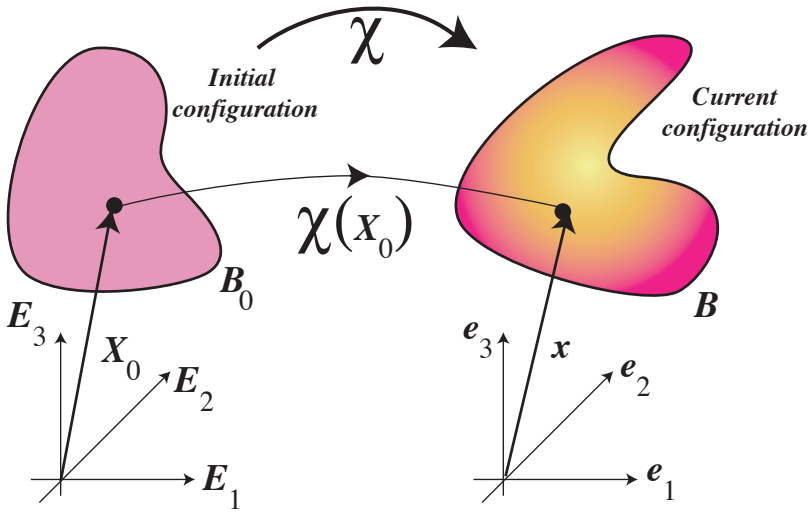

Figure 30: Basic kinematic of nonlinear elasticity. Two configurations are defined (with possibly different sets of coordinates). The deformation is a 1-1 map between points of the reference configuration $\mathcal{B}_0$ and points of the current configuration $\mathcal{B}$.

bases to represent vectors in the initial and current configuration

$$\mathbf{x} = x_i \mathbf{e}_i, \qquad \mathbf{X}_0 = X_{0,i} \mathbf{E}_i, \tag{56}$$

where summation over repeated indices is assumed. The natural choice of representation in solid mechanics for the relevant geometric and physical quantities (deformation gradient, stresses) are tensors. The tensor product of two vectors $\mathbf{u} \otimes \mathbf{v}$ of two vectors $\mathbf{u}$ and $\mathbf{v}$ is a tensor such that

$$(\mathbf{u} \otimes \mathbf{v})\mathbf{a} = (\mathbf{v} \cdot \mathbf{a})\mathbf{u}, \tag{57}$$

where $(\mathbf{v} \cdot \mathbf{a})$ denotes the scalar product between the two vectors. In components, $\mathbf{u} = u_i \mathbf{e}_i$ and $\mathbf{v} = v_i \mathbf{e}_i$ so that $\mathbf{u} \otimes \mathbf{v} = u_i \mathbf{e}_i = u_i v_j \mathbf{e}_i \otimes \mathbf{e}_j$. In general, denoting the

components of a tensor in a basis $\{\mathbf{e}_i\}$, we have

$$\mathbf{T} = T_{ij}\mathbf{e}_i \otimes \mathbf{e}_j \qquad \Longleftrightarrow \qquad T_{ij} = \mathbf{e}_i \cdot \mathbf{T}\mathbf{e}_j, \tag{58}$$

we have $(\mathbf{u} \otimes \mathbf{v})_{ij} = u_i v_j$. If we define the matrix of components by $[T_{ij}]$, most linear algebra identities and definitions carry readily over to tensors, for instance,

$$\det \mathbf{T} = \det([T_{ij}]) \qquad \text{tr } \mathbf{T} = \text{tr } ([T_{ij}]) \tag{59}$$

and $\mathbf{T}^{\mathrm{T}} = \mathbf{T} \iff T_{ij} = T_{ji}$. Similarly, the product of two tensors $\mathbf{ST}$ is defined as $(\mathbf{ST})\mathbf{v} = \mathbf{S}(\mathbf{T}\mathbf{v})$ and, not surprisingly, $[ST] = [S][T]$.

Next, we define derivatives of scalar, vector, and tensorial fields. Let ϕ, u, $\mathbf{T}$ be scalar, vector and tensor fields respectively over $\mathbf{x}$, that is

$$\phi = \phi(\mathbf{x}), \qquad \mathbf{u} = u_i(\mathbf{x})\mathbf{e}_i, \qquad \mathbf{T} = T_{ij}(\mathbf{x})\mathbf{e}_i \otimes \mathbf{e}_j. \tag{60}$$

We define first the gradient of a scalar and vector by, that is

$$\text{grad } \phi = \frac{\partial \phi}{\partial \mathbf{x}} = \frac{\partial \phi}{\partial x_i}\mathbf{e}_i, \tag{61}$$

$$\text{grad } \mathbf{u} = \frac{\partial \mathbf{u}}{\partial \mathbf{x}} = \frac{\partial \mathbf{u}}{\partial x_j} \otimes \mathbf{e}_j = \frac{\partial (u_i \mathbf{e}_i)}{\partial x_j} \otimes \mathbf{e}_j = \frac{\partial u_i}{\partial x_j}\mathbf{e}_i \otimes \mathbf{e}_j. \tag{62}$$

The gradient above is defined as the operation $\text{grad}(\ \cdot\ ) = \frac{\partial (\ \cdot\ )}{\partial x_j} \otimes \mathbf{e}_j$. Similarly, we define the gradient of a tensor by

$$\text{grad } \mathbf{T} = \frac{\partial}{\partial x_k}(T_{ij}\mathbf{e}_i \otimes \mathbf{e}_j) \otimes \mathbf{e}_k = \frac{\partial T_{ij}}{\partial x_k}\mathbf{e}_i \otimes \mathbf{e}_j \otimes \mathbf{e}_k \tag{63}$$

And we define the divergence by contracting tensors,

$$\text{div } \mathbf{T} = \frac{\partial T_{ij}}{\partial x_k}\mathbf{e}_j\,(\mathbf{e}_i \cdot \mathbf{e}_j) = \frac{\partial T_{ij}}{\partial x_i}\mathbf{e}_j. \tag{64}$$

We can now introduce the central geometric object of nonlinear elasticity that describes locally relative deformations, the *deformation gradient* obtained as the spatial derivative of the mapping $\boldsymbol{\chi}$. Given a vector $\mathbf{x} = x_i(\mathbf{X}_o)\mathbf{e}_i$, the deformation gradient tensor is $\mathbf{F} = \text{Grad}\boldsymbol{\chi}$, that is

$$\mathbf{F} = \frac{\partial}{\partial X_{0,j}}(x_i \mathbf{e}_i) \otimes \mathbf{E}_j = \frac{\partial x_i}{\partial X_{0,j}}\mathbf{e}_i \otimes \mathbf{E}_j \equiv F_{ij}\mathbf{e}_i \otimes \mathbf{E}_j. \tag{65}$$

Note that the bases in which the gradient is taken are mixed. Geometrically, $\mathbf{F}$ is a linear map that transforms a vector $\mathbf{v}$ at a point $p \in \mathcal{B}_0$ to a vector $\mathbf{F}\mathbf{v}$ at the same material point but in the current configuration (See Fig. 31).

It is standard to show [120] that the determinant $J = \det \mathbf{F} > 0$ of the deformation gradient represents the local change of volume, that is the image of an infinitesimal volume element $\mathrm{d}v$ at a material point p is $\mathrm{d}v = J\mathrm{d}V$.

Similarly, it can be shown that an infinitesimal element of area defined in the reference configuration by a normal $\mathbf{N}$ and surface area $\mathrm{d}A$ is transformed into another

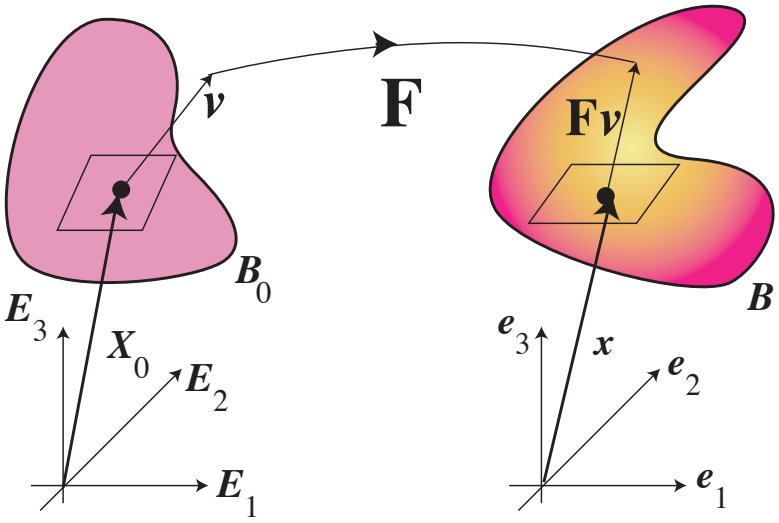

Figure 31: The deformation gradient maps vectors on the tangent space at a material point in the initial configuration to vectors in the tangent space in the current configuration at the same material point.

element of area in the current configuration defined by a vector $\mathbf{n}$ with area $\mathrm{d}a$ and related to the reference one by Nanson's formula, that is

$$\mathbf{n}\mathrm{d}a = J\mathbf{F}^{-T}\mathbf{N}\mathrm{d}A \tag{66}$$

Now consider a local infinitesimal vector $\mathrm{d}\mathbf{X}$ tangent to a material line in $\mathcal{B}_0$ at p, then its image $\mathrm{d}\mathbf{x} = \mathbf{F}\mathrm{d}\mathbf{X}_0$. If $\mathbf{M}$ is the unit vector along $\mathrm{d}\mathbf{X}_0$ then

$$\mathrm{d}\mathbf{X}_0 = \mathbf{M}\,\mathrm{d}S_0 = \mathbf{M}|\mathrm{d}\mathbf{X}_0| \quad \text{and} \quad \mathrm{d}\mathbf{x} = \mathbf{m}\,\mathrm{d}s = \mathbf{m}|\mathrm{d}\mathbf{x}| \tag{67}$$

which implies that $\mathbf{m}\,\mathrm{d}s = \mathbf{F}\mathbf{M}\,\mathrm{d}s$. Now take the norm of each side:

$$|\mathrm{d}s|^2 = (\mathbf{F}\mathbf{M}\cdot\mathbf{F}\mathbf{M})|\mathrm{d}S_0|^2 = (\mathbf{F}^T\mathbf{F}\mathbf{M})\cdot\mathbf{M}|\mathrm{d}S_0|^2 \tag{68}$$

$$\iff \frac{\mathrm{d}s}{\mathrm{d}S_0} = \sqrt{(\mathbf{F}^T\mathbf{F}\mathbf{M})\cdot\mathbf{M}} \equiv \lambda(M), \tag{69}$$

where $\mathrm{d}s/\mathrm{d}S_0$ is the change of length of a material line in the direction $\mathbf{M}$ and λ is a stretch. This implies that the material is unstrained in the direction $\mathbf{M}$ if and only if $\lambda(\mathbf{M}) = 1$. We also see the appearance of an important tensor to describe strain in a body, namely, the right Cauchy-Green tensor

$$\mathbf{C} = \mathbf{F}^T\mathbf{F}, \tag{70}$$

and a material is *unstrained* if $\mathbf{C} = \mathbf{1}$. Geometrically, it can be seen that $\mathbf{C}$ is a metric on $\mathcal{B}$ as it provides a way to measure distances and angles on the new body (See Section **??**).

4.2 Balance of mass

Next to describe a material, we attach physical properties to our continuum. We define a scalar field $\rho = \rho(\mathbf{x}, t)$, the *volume density* at each point of the body in its current configuration and assume that mass is conserved, which leads to the usual continuity equation for the evolution of density [121]

$$\dot{\rho} + \rho \operatorname{div} \mathbf{v} = 0. \tag{71}$$

4.3 Balance of linear and angular momentum

The forces distributed on a body $\mathcal{B}$ include a contact-force density $\mathbf{t}_n$ and a body-force density $\mathbf{b}$. In accordance with Euler's laws of motion [122], the balance of linear momentum is

$$\int_{\mathcal{B}_f} \rho(\mathbf{x}, t)\mathbf{b}(\mathbf{x}, t)\mathrm{d}v + \int_{\partial\mathcal{B}_f} \mathbf{t}_n \mathrm{d}a = \int_{\mathcal{B}_f} \rho(\mathbf{x}, t)\dot{\mathbf{v}}(\mathbf{x}, t)\mathrm{d}v, \tag{72}$$

where $\dot{\mathbf{v}}$ is the time derivative of the velocity vector such that $\mathbf{v}(\mathbf{x}, t) = \dot{\chi}(\mathbf{X}_0, t)$. According to Cauchy's theorem, the contact-force density depends linearly on the unit normal $\mathbf{n}$, given by $\mathbf{t}_n = \mathbf{T}\mathbf{n}$, where $\mathbf{T}$ is referred to as the Cauchy stress tensor. Using Cauchy's theorem and applying the divergence theorem to (72) yields the equilibrium equation

$$\operatorname{div}(\mathbf{T}^{\mathrm{T}}) + \rho\mathbf{b} = \rho\dot{\mathbf{v}}. \tag{73}$$

Balancing the moments of the forces acting on the body $\mathcal{B}$ reveals that the stress tensor is symmetric, that is $\mathbf{T}^{\mathrm{T}} = \mathbf{T}$ and we obtain Cauchy's equation for the balance of stress:

$$\operatorname{div}(\mathbf{T}) + \rho\mathbf{b} = \rho\dot{\mathbf{v}}, \tag{74}$$

where the divergence is taken with respect to $\mathbf{x}$ in the current configuration. The solutions to the equilibrium equations must satisfy the conditions imposed on the boundary which can be in the form of dead-loading, rigid-loading, or mixed-loading. Dead-loading prescribes the components of the stresses at the boundary, rigid-loading imposes a fixed deformation at the boundary, and mixed-loading imposes fixed deformations on some part of the body and stresses on the remaining boundary.

4.4 Constitutive equations

We assume that the body is hyperelastic. That is, the material can be described by a strain-energy function $W = W(\mathbf{F})$ and the Cauchy stress is related to the elastic deformation by

$$\mathbf{T} = J^{-1}\mathbf{F}\frac{\partial W}{\partial \mathbf{F}} - p\mathbf{1}, \tag{75}$$

where p is a Lagrange multiplier associated with the internal constraint of incompressibility and $J = \det(\mathbf{F})$ as before. For an incompressible material, $J = 1$ and p is the hydrostatic pressure. If the material is compressible, then $p = 0$.

If we restrict our attention to isotropic materials, we can write the strain-energy function either in terms of the principal stretches λ_1, λ_2, λ_3 (the square roots of the

principal values of $\mathbf{F}\mathbf{F}^{\mathrm{T}}$) or, equivalently, in terms of the first three principal invariants of the Cauchy-Green strain tensors, given by

$$I_1 = \mathrm{tr}(\mathbf{C}) = \lambda_1^2 + \lambda_2^2 + \lambda_3^2, \tag{76}$$

$$I_2 = \frac{1}{2}\left(I_1^2 - \mathrm{tr}(\mathbf{C}^2)\right) = \lambda_2^2\lambda_3^2 + \lambda_3^2\lambda_1^2 + \lambda_1^2\lambda_2^2 \tag{77}$$

$$I_3 = \det(\mathbf{C}) = \lambda_1^2\lambda_2^2\lambda_3^2, \tag{78}$$

and we write $W = W(I_1, I_2, I_3)$ for an isotropic compressible material and $W = W(I_1, I_2)$ for an isotropic incompressible material. The explicit form of the Cauchy stress tensor in terms of the invariants and their derivatives is

$$\mathbf{T} = w_0\mathbf{1} + w_1\mathbf{B} + w_2\mathbf{B}^2 \tag{79}$$

where $\mathbf{B} = \mathbf{F}\mathbf{F}^{\mathrm{T}}$ is the left Cauchy-Green tensor and

$$w_0 = 2\frac{\partial W}{\partial I_3} - p, \quad w_1 = 2J^{-1}\frac{\partial W}{\partial I_1} + 2J^{-1}\frac{\partial W}{\partial I_2}I_1, \quad w_2 = -2J^{-1}\frac{\partial W}{\partial I_2}$$

As before we choose $p = 0$ for compressible materials and $J = I_3 = 1$ for incompressible ones.

4.5 Choice of strain-energy density function

The choice of strain-energy density functions for elastomers and soft-tissues $W = W(\mathbf{F})$ is a controversial and difficult problem. Typically, phenomenological models are used to capture the essential features of the material (its behaviour under shear or its strain-hardening or strain-softening properties), while respecting basic material properties such as convexity and material-frame indifference. A few key popular models that capture specific features and are widely used are given in Table 1).

4.6 Summary of equations

We can now collect the different equations from the previous chapters to obtain a closed set of equations

$$\dot{\rho} + \rho\mathrm{div}\ \mathbf{v} = 0, \qquad \text{mass conservation} \tag{80}$$

$$\mathrm{div}\ \mathbf{T} + \rho\mathbf{b} = \rho\dot{\mathbf{v}}, \qquad \text{linear momentum conservation} \tag{81}$$

$$\mathbf{T}^{\mathrm{T}} = \mathbf{T}, \qquad \text{angular momentum conservation} \tag{82}$$

$$\mathbf{T} = J^{-1}\mathbf{F}\frac{\partial W}{\partial \mathbf{F}} - p\mathbf{1} \qquad \text{constitutive law} \tag{83}$$

Since the elements of $\mathbf{F}$ are related to the motion $\boldsymbol{\chi}$ by $\mathbf{F} = \mathrm{Grad}\boldsymbol{\chi}$, and $\mathbf{v} = \partial_t\boldsymbol{\chi}(\mathbf{x}, t)$, there are 10 unknowns left: 1 in ρ, 3 in vector $\boldsymbol{\chi}$ and 6 in the symmetric tensor $\mathbf{T}$ for 10 equations (excluding the third equation that reduces the number of unknowns in $\mathbf{T}$).

Name	Definition	soft tissues	elastomers
neo-Hookean	$W_{\rm nh} = \dfrac{\mu}{2}(I_1 - 3)$		
Mooney-Rivlin	$W_{\rm mr} = \mu\dfrac{(I_1-3)+\nu(I_2-3)}{2(1+\nu)}$		
1-term Ogden	$W_{\rm og} = \dfrac{2\mu}{\beta^2}(\lambda_1^\beta + \lambda_2^\beta + \lambda_3^\beta - 3)$	$\beta \geq 9$	$\beta \approx 3$
Fung	$W_{\rm fu} = \dfrac{\mu}{2\beta}[\exp\beta(I_1-3) - 1]$	$3 < \beta < 20$	
Gent	$W_{\rm ge} = -\dfrac{\mu}{2\beta}\log[1-\beta(I_1-3)]$	$0.4 < \beta < 3$	$0.005 < \beta < 0.05$

Table 1: A list of strain-energy functions. Note that the materials have been written so that they share the same infinitesimal shear modulus μ. The limits $\nu \to 0$, $\beta \to 2$ in Ogden and, $\beta \to 0$ in Fung and Gent all lead to the neo-Hookean potential. Estimates are taken from: 1-term Ogden is [123, 124], Gent [125, 126, 127, 128], Fung [129, 130].

4.6.1 An example: the inflation of an incompressible cylinder

As an illustrative example, we consider the classical problem of an incompressible hyperelastic cylindrical shell subject to inflation [131]. The tube of initial inner radius A_0 and outer radius $B_0 > A_0$ is deformed into a tube with radii a, b and the same height. We consider a finite deformation in which the cylinder is allowed to inflate and extend while remaining cylindrical at all time irregardless of possible stability issues [132]. The deformation $\mathbf{x} = \boldsymbol{\chi}(\mathbf{X}_0, t)$, in cylindrical coordinates reads

$$r = r(R_0), \quad \theta = \Theta_0, \quad z = Z_0, \tag{84}$$

so that the position vectors are (respectively)

$$\mathbf{X}_0 = R_0\mathbf{E}_R + Z_0\mathbf{E}_Z, \quad \mathbf{x} = r(R_0)\mathbf{e}_r + Z_0\mathbf{e}_z. \tag{85}$$

The deformation gradient in cylindical coordinates is thus given by

$$\mathbf{F} \equiv \mathrm{diag}(\lambda_r, \lambda_\theta, \lambda_z) = \mathrm{Grad}(\boldsymbol{\chi}) = \mathrm{diag}(r', r/R_0, 1), \tag{86}$$

where the gradient is taken in the initial reference configuration, the prime denotes differentiation with respect to R_0. Using the incompressibility condition $\det(\mathbf{F}) = 1$ leads to $r'r = R_0$ that is $r = \sqrt{a^2 + R_0^2 - A_0^2}$ and $\lambda = \lambda_\theta$ is given by

$$\lambda = \frac{r}{R_0} = \frac{1}{R_0}\sqrt{a^2 + R_0^2 - A_0^2}. \tag{87}$$

Therefore the deformation is fully specified by the radial stretch of the inner wall $\lambda_a = a/A_0$: once a is known the outer radius is determined by inserting $r = b$, $R_0 = B$ in (87).

Since the deformation is diagonal in cylindrical coordinates and only depends on R_0, it follows from Eq. (79) that the Cauchy stress tensor is also diagonal in these coordinates so that $\mathbf{T} \equiv \mathrm{diag}(t_r, t_\theta, t_z)$. We consider a simple thought experiment in which the tube inflates due to an internal pressure P. Taking $t_r(r = b) = 0$, the two boundary condition is

$$t_r(r = a) = -P, \quad t_r(r = b) = 0 \tag{88}$$

This relates the radial stress to the pressure jump across the tube wall.

Note that the Cauchy equation $\mathrm{div}\,\mathbf{T} = 0$ in cylindrical coordinates leads to a single scalar equation

$$\frac{dt_r}{dr} + \frac{1}{r}(t_r - t_\theta) = 0. \tag{89}$$

To close the system, we also have the constitutive law:

$$t_r = \lambda_r \frac{\partial W}{\partial \lambda_r} - p, \quad t_\theta = \lambda_\theta \frac{\partial W}{\partial \lambda_\theta} - p. \tag{90}$$

We now proceed to construct a solution in the case of a neo-Hookean strain energy.

Inflation of a neo-Hookean cylinder

Thus the deformation is determined by finding the value of a satisfying

$$P = \mu \int_A^B \frac{\lambda(R)^2 - \lambda(R)^{-2}}{r(R)^2} R\, dR := f(a) \tag{91}$$

5 Volumetric growth

Overview

Having introduced the general elastic and kinematic equation in the absence of growth, we can now develop a general theory for growing material based on the same decomposition as the one we introduced in one dimension.

5.1 Kinematics of growth: The multiplicative decomposition

The existence of residual stress in biological materials can be attributed and described through a growth process. As different elements of a body change in size, they create stresses independently of the applied loads. The main postulate of morphoelasticity is that residual stresses are solely created by a local growth deformation tensor mapping the initial reference configuration to a new virtual reference configuration $\mathcal{V}$. This tensor describes locally the change of shape and volume at all points in the body due to growth.

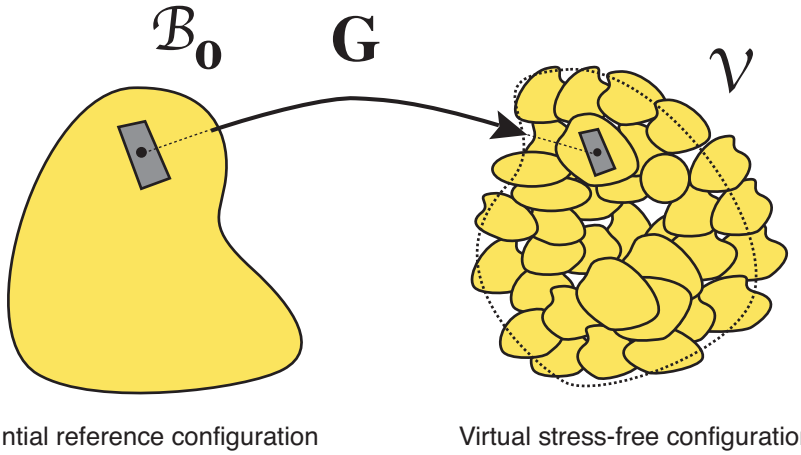

Figure 32: The action of the growth tensor. The growth tensor maps vectors in the tangent space of the initial configuration to vectors in the tangent space of the virtual configuration. Both configurations are stress-free.

The second step in the process is to map the virtual configuration back to Euclidean space by introducing an elastic deformation at each point. This map $\mathbf{A}_r$ ensures the integrity and compatibility of the body so that

$$\mathbf{F}_r(\mathbf{X}_0, t) = \mathbf{A}_r(\mathbf{X}_0, t)\mathbf{G}(\mathbf{X}_0, t). \tag{92}$$

is a local deformation gradient between two compatible configurations of the same body B. By construction $\mathbf{F}_r$ is the gradient of an invertible differentiable map between the initial reference configuration and the residually stressed configuration

$$\mathbf{x}_r = \boldsymbol{\chi}_r(\mathbf{X}_0, t), \tag{93}$$

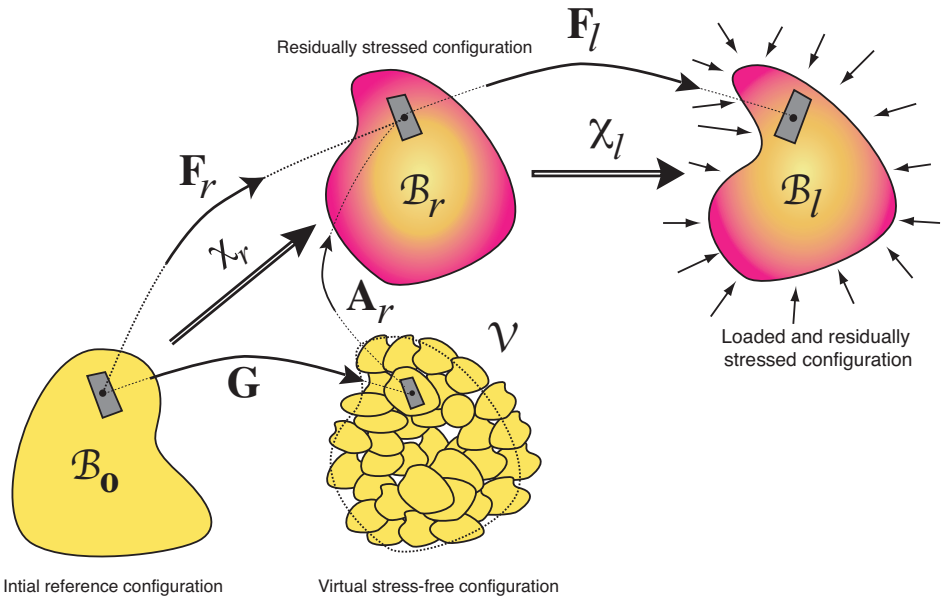

Figure 33: The creation of residual stress

where $\mathbf{x}_r$ denotes the position of a point p in the current configuration with position $\mathbf{X}_0$ in the initial reference configuration (Fig. 33). Finally, if one is interested in the deformation of the grown body under loads, an extra step mapping the residually stressed configuration to the loaded current configuration is considered

$$\mathbf{F}_l : \mathrm{T}\mathcal{B}_r \to \mathrm{T}\mathcal{B}. \tag{94}$$

Physically the two elastic steps $\mathbf{A}_r$ and $\mathbf{F}_l$ in the growth process can be thought of as the local shrinking, growing, and rigid-body motion of the dislocated sub-bodies associated with $\mathcal{V}$ so that they again form a compatible configuration and match the external loads. These two steps can be written as a single elastic step

$$\mathbf{A} = \mathbf{F}_l\mathbf{A}_r : \mathrm{T}\mathcal{V} \to \mathrm{T}\mathcal{B}. \tag{95}$$

Doing so, we can view growth as the the following two steps: first, the growth tensor $\mathbf{G}$ takes the initial configuration to a virtual stress-free configuration, possibly incompatible. Second, a local elastic tensor $\mathbf{A}$ restores compatibility of the body and enforces the boundary conditions so that the body is in a compatible configuration and in mechanical equilibrium. That is, we have

$$\mathbf{F}(\mathbf{X}, t) = \mathbf{A}(\mathbf{X}, t)\mathbf{G}(\mathbf{X}, t), \tag{96}$$

where both $\mathbf{A}$ and $\mathbf{G}$ have strictly positive determinants.

5.2 Elastic constitutive laws

To describe the elastic deformation, a constitutive law is needed again to relate the stress to the deformation. We will assume again that the material as it grows remains hyperelastic. However, the reference configuration for elastic deformation (that is the

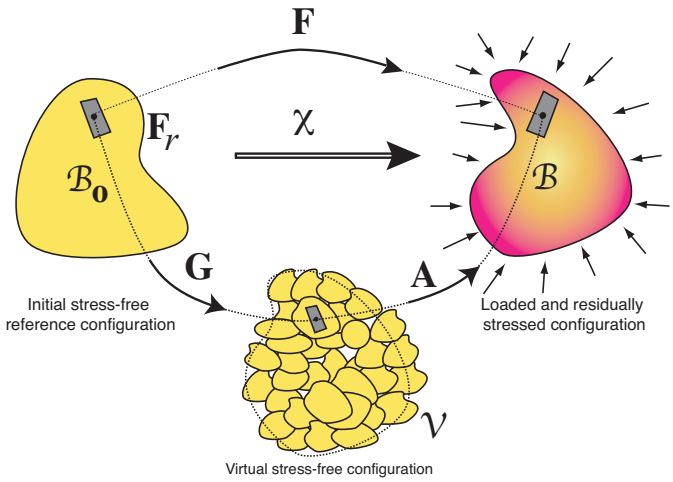

Figure 34: The multiplicative-decomposition

configuration in which no deformation leads to no stress) is not the initial configuration but the virtual configuration. Therefore, the elastic energy depends only on the elastic deformation tensor $\mathbf{A}$, so that $W = W(\mathbf{A})$ and the stresses are then given by

$$\mathbf{T} = J_A^{-1}\mathbf{A}\frac{\partial W}{\partial \mathbf{A}} - p\mathbf{1} \tag{97}$$

where W is the strain energy function. If the material is elastically incompressible, $J_A = 1$ and p is the hydrostatic pressure; for an elastically compressible material $p = 0$.

5.3 Particular forms and symmetry of the growth tensor

In many problems, it is useful to restrict the form of the growth tensor. Similar to the decomposition used to describe material symmetries, we can use general tensorial form of increasing complexity to describe growth process occurring with a prescribed symmetry.

- **Isotropic growth.** The simplest non trivial form for the growth tensor is to take it as multiple of the identity, that is

$$\mathbf{G} = g\mathbf{1}. \tag{98}$$

  In such case, we have $J_G = g^3$ representing the isotropic change of a volume. It can be shown that a theory of multiplicative decomposition is not really needed in the sense that the effect of growth can be completely taken into account through a proper definition of the determinant of $\mathbf{F}$ as is customary in the theory of swelling gels [133].

- **Bi-directional growth.** A rather useful and general way to describe growth is to identify two direction in which growth can take place differentially. That is,

in the initial configuration, we identify two unit vectors $\mathbf{g}_1$ and $\mathbf{g}_2$ and introduce the particular (but rather large) class of growth tensors

$$\mathbf{G} = g_0\mathbf{1} + (g_1 - 1)\mathbf{g}_1 \otimes \mathbf{g_1} + (g_2 - 1)\mathbf{g}_2 \otimes \mathbf{g}_2. \tag{99}$$

where g_0 represents the isotropic part of the growth process and g_1 and g_2 the anisotropic parts. The advantage of such a representation is that it reduces the number of growth descriptors to three functions for the increase in volume and two unit vectors for the directions in which growth takes place anisotropically. Further restrictions of this growth tensor are also of interest.

- **Transversely isotropic growth.** In transverse isotropic growth, we assume that, locally, growth takes place both isotropically and in a given direction characterised by a single unit vector $\mathbf{g}$ so that

$$\mathbf{G} = g_0\mathbf{1} + (g_1 - 1)\mathbf{g} \otimes \mathbf{g}. \tag{100}$$

This description of growth is particularly useful for fibre-reinforced system with growth along the fibres.

Note that in the forms above, there is also a distinction between **homogeneous growth**, for which the growth is independent of position, and **heterogeneous growth**, in which the growth varies with position.

5.4 The growing ring

As an illustrative example, we return to the inflation of an incompressible cylindrical tube (without extension) due to an internal pressure, but with added radial and circumferential growth. That is, we assume the growth tensor has the form $\mathbf{G} = \mathrm{diag}(\gamma_r, \gamma_\theta, 1)$, where γ_r corresponds to radial growth and γ_θ to circumferential growth.

The deformation gradient tensor, expressed in cylindrical coordinates, is $\mathbf{F} = \mathrm{diag}(r'(R_0), r/R_0, 1)$. The elastic strain tensor is $\mathbf{A} = \mathrm{diag}(\alpha_r, \alpha_\theta, 1)$. Since $\mathbf{F} = \mathbf{AG}$, we have

$$\alpha_r = \frac{r'}{\gamma_r}, \quad \alpha_\theta = \frac{r}{R_0\gamma_\theta}. \tag{101}$$

Material incompressibility implies $\det\mathbf{A} = 1$, that is $\alpha_r\alpha_\theta = 1$ which implies $rdr = R_0 g(R_0)dR_0$, that is

$$r^2 = a^2 + 2\int_{A_0}^{R_0} g(\rho)\rho d\rho \tag{102}$$

where $g(R_0) = \det\mathbf{G} = \gamma_r\gamma_\theta$.

In the reference configuration, the equilibrium conditions have not been modified from the ones derived in Example 4.6.1. They are still given by the first non-vanishing Cauchy equations $\frac{dt_r}{dr} + \frac{1}{r}(t_r - t_\theta) = 0$ and the applications of the boundary condition

$$\int_a^b \frac{t_\theta - t_r}{r} dr = P \tag{103}$$

The difficulty is that the bounds of the integrals a and b are functions of the growth terms γ_i. It is therefore simpler to reformulate these integrals in the initial configuration.

Inflation of a growing neo-Hookean cylinder

Thus the deformation is determined by finding the value of a satisfying

$$P = \mu \int_A^B \frac{\alpha(R)^2 - \alpha(R)^{-2}}{r(R)^2} \gamma_r \gamma_\theta R \, dR := f(a) \tag{104}$$

If growth is chosen to be transversely isotropic ($\gamma_r = \gamma_\theta$), no residual stress is created and the new ring is a dilation of the original one, that is $r = \gamma_r R_0$. If however we consider anisotropic homogeneous growth ($\gamma_r \neq \gamma_\theta$), then residual stress is created as shown in Fig. 35B where excess of radial growth with respect to hoop growth induces a compressive residual radial stress in the material. In terms of the hoop stress, the inner radius is in compression while the outer radius is in tension. Circumferential growth, or equivalently radial resorption, creates a tensile radial stress, this is the case $\gamma_r < 1$ (not shown). Next, we consider hoop stress in the material when $P < 0$ (internal pressure) as shown in Fig. 35C. In the absence of growth, one observes a steep profile as a function of R_0 whereas with suitable growth, this profile completely flattens. It is this simple but crucial observation that first indicated that residual stress could play an important role in physiology. Indeed, in arteries, the residual stress acts very much in the same way suggesting that differential growth in arteries could take place to reduce gradients of hoop stress preventing material failure associated with tissue separation

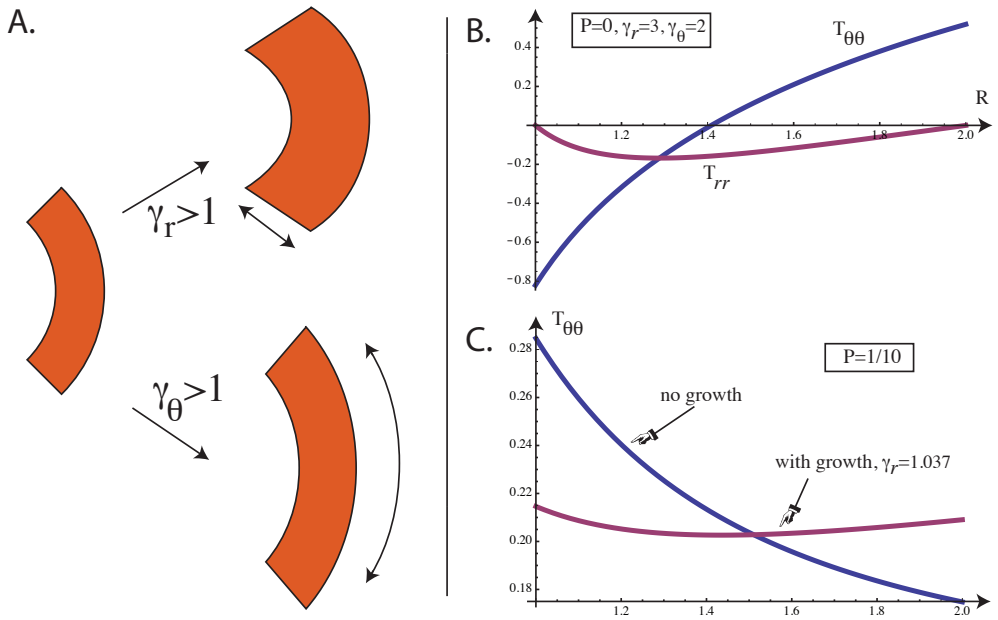

Figure 35: A: Growth of disk elements. A disk sector remains a disk sector when either grown through hoop only growth and/or radial growth. B: Residual stress due to growth. Even in the absence of loads, both radial and hoop growth are chosen and result in a compressive radial stress and non-vanishing hoop stress. C: Under pressure and in the absence of residual stress, large hoop stress gradients are observed. With appropriate growth, the hoop stress profile flattens out. (In both cases $\mu = 1$ is chosen without loss of generality).

[134, 84, 135].

5.4.1 The opening-angle method

The growth of a ring and the residual stress it generates can be directly observed by cutting the ring and observing that it relaxes to a sector as shown schematically in Fig. 36 and experimentally in Fig. 16 for arteries. In the present case, assuming again an homogeneous body and no deformation in the axial direction and if we further assume that the open body has the shape of a ring sector and that it is stress free, then the residual stress can be fully described by the geometry of this open configuration and a suitable growth tensor can be identified. Indeed, in such cases, the virtual configuration is locally compatible and is, for positive opening-angles, globally compatible too. Therefore, we can find a set of coordinates describing the body and an invertible mapping between the initial and virtual configuration given by

$$R = R_0, \quad \Theta = \varphi + (1 - \varphi/\pi)\Theta_0, \quad Z = Z_0, \tag{105}$$

and choose without loss of generality $A = A_0$, $B = B_0$. The growth tensor is then easily identified, in cylindrical coordinates, as

$$\mathbf{G} = \mathrm{diag}(1, \varphi/\pi, 1). \tag{106}$$

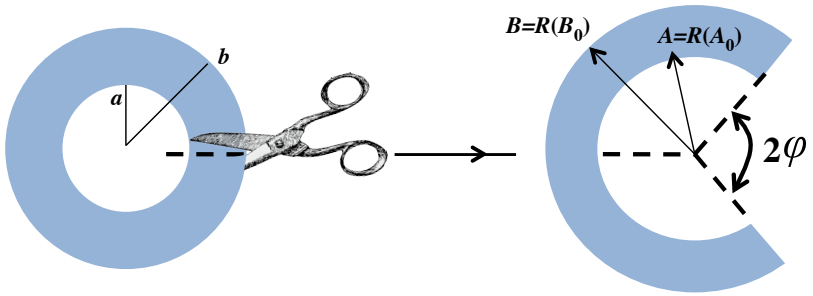

Figure 36: Schematic of a radial cut in an ring and the corresponding opening angle φ.

Once the growth tensor is known, the stress field of the closed disk under load can be calculated as before.

References

[1] J. S. Langer. Instabilities and pattern-formation in crystal-growth. *Rev. Mod. Phys.*, 52, 1980.

[2] A. Boudaoud and S. Chaïeb. Mechanical phase diagram of shrinking cylindrical gels. *Phys. Rev. E*, 68(2):21801, 2003.

[3] H. R. Duhamel du Monceau. La physique des arbres (The physics of trees). *L. Guérin et L. -F. Delatour, Paris, France*, 1758.

[4] M. O. Reinhardt. Das wachsthum der pilzhyphen. *Jahrbücher für wissenschaftliche botanik*, 23, 1892.

[5] D'Arcy W. Thomspon. *On Growth and Form: The Complete Revised Edition*. Dover, New York, 1992.

[6] D. E. Moulton and A. Goriely. Surface growth kinematics via local curve evolution. *J. Math. Biol.*, 68(1-2):81–108, 2014.

[7] Richard E Scammon. The first seriatim study of human growth. *Am. J. Phys. Anthrop.*, 10(3):329–336, 1927.

[8] Carl Heinrich Stratz. *Naturgeschichte des Menschen*. F. Enke, 1904.

[9] S. A. Stewart and R. Z. German. Sexual dimorphism and ontogenetic allometry of soft tissues in rattus norvegicus. *J. Morphology*, 242(1):57–66, 1999.

[10] Adolphe Quetelet. *Sur l'homme et le développement de ses facultés ou essai de physique sociale*. Bachelier, 1835.

[11] K Devlin. Do you believe in fairies, unicorns, or the BMI? *Mathematical Association of America*, 2009.

[12] J. S. Huxley and G. Teissier. Terminology of relative growth. *Nature*, 137(3471):780–781, 1936.

[13] Henry H Donaldson. A comparison of the albino rat with man in respect to the growth of the brain and of the spinal cord. *J. Comp. Neurol. Psych.*, 18(4):345–392, 1908.

[14] Barry Bogin. *Patterns of human growth*, volume 23. Cambridge University Press, 1999.

[15] A. Putter. Studien über physiologische Ähnlichkeit. vi. *Wachstumsahmlichkeiten. Pflagers. Arch. Gres. Physiol*, 180:298–340, 1920.

[16] L. Von Bertalanffy. Quantitative laws in metabolism and growth. *Q. Rev. Biol.*, 32(3):217–231, 1957.

[17] A Tsoularis and J Wallace. Analysis of logistic growth models. *Math. Bisoc.*, 179(1):21–55, 2002.

[18] FJ Richards. A flexible growth function for empirical use. *J. Exp. Bot.*, 10(2):290–301, 1959.

[19] F Sarrus and JF Rameaux. Application des sciences accessoires et principalement des mathématiques à la physiologie générale. *Bulletin de l'Académie Royale Médecine, Paris*, 3:1094–1100, 1839.

[20] Geoffrey B West, James H Brown, and Brian J Enquist. A general model for ontogenetic growth. *Nature*, 413(6856):628–631, 2001.

[21] Max Kleiber. Body size and metabolic rate. *Physiol. Rev*, 27(4):511–541, 1947.

[22] Karl J Niklas. Plant allometry: is there a grand unifying theory? *Biol. Rev.*, 79(4):871–889, 2004.

[23] AA Heusner. Energy metabolism and body size I. Is the 0. 75 mass exponent of Kleiber's equation a statistical artifact? *Respiration Physiol.*, 48(1):1–12, 1982.

[24] Geoffrey B West, James H Brown, and Brian J Enquist. A general model for the origin of allometric scaling laws in biology. *Science*, 276(5309):122–126, 1997.

[25] R Darrell Bock, Howard Wainer, Anne Petersen, David Thissen, James Murray, and Alex Roche. A parameterization for individual human growth curves. *Human Biology*, 45(1):63–80, 1973.

[26] P. B. Medawar. The laws of biological growth. *Nature*, 148(3665):772–774, 1941.

[27] Benjamin Gompertz. On the nature of the function expressive of the law of human mortality, and on a new mode of determining the value of life contingencies. *Phil. Trans. R. Soc. Lond.*, 115:513–583, 1825.

[28] Charles P Winsor. The Gompertz curve as a growth curve. *Proc. Natl. Acad. Sci. USA*, 18:1–8, 1932.

[29] MH Zwietering, Il Jongenburger, FM Rombouts, and K Van't Riet. Modeling of the bacterial growth curve. *Appl. Environ. Microb.*, 56(6):1875–1881, 1990.

[30] Thomas R Alley. Head shape and the perception of cuteness. *Developmental Psychology*, 17(5):650–654, 1981.

[31] K. Lorenz. Part and parcel in animal and human societies. *Studies in animal and human behavior*, 2:115–195, 1971.

[32] T. Cabana, P. Jolicoeur, and J. Michaud. Prenatal and postnatal growth and allometry of stature, head circumference, and brain weight in Québec children. *Am. J. Human Biol.*, 5(1):93–99, 1993.

[33] J. S. Huxley, J. Needham, and I. M. Lerner. Terminology of relative growth-rates. *Nature*, 148:225, 1941.

[34] C. F. Stevens. Darwin and Huxley revisited: the origin of allometry. *J. Biol.*, 8:14, 2009.

[35] C. Champy. Sexualité et hormones. *Paris: Gaston Doin*, 1924.

[36] Jean Gayon. History of the concept of allometry. *American Zoologist*, 40(5):748–758, 2000.

[37] E. Dubois. Sur le rapport du poids de l'encéphale avec la grandeur du corps chez les mammifères. *Bulletins de la Socité d'Anthropologie de Paris*, 8(1):337–376, 1897.

[38] L. Lapicque. Sur la relation du poids de l'encéphale aux poids du corps. *Comptes Rendus Séances Soc. Biol. Fil. ,(Sér 10)*, 5:62–63, 1898.

[39] Paul Broca. *Sur le volume et la forme du cerveau suivant les individus et suivant les races*, volume 1. Hennuyer, 1861.

[40] Julian Huxley. *Problems of relative growth*. Methuen, 1932.

[41] J. F. White and S. J. Gould. Interpretation of the coefficient in the allometric equation. *Am. Nat.*, pages 5–18, 1965.

[42] D. Pilbeam and S. J. Gould. Size and scaling in human evolution. *Science*, 186:892–901, 1974.

[43] E. R. Weibel. Physiology: the pitfalls of power laws. *Nature*, 417(6885):131–132, 2002.

[44] Karl J Niklas. *Plant Allometry: the Scaling of Form and Process*. University of Chicago Press, 1994.

[45] J. Sachs. *Text-book of botany, morphological and physiological*. Clarendon, Oxford, 1875.

[46] Gyung-Tae Kim and Kiu-Hyung Cho. Recent advances in the genetic regulation of the shape of simple leaves. *Physiologia Plantarum*, 126(4):494–502, 2006.

[47] Russell T Turner. Invited review: what do we know about the effects of spaceflight on bone? *J. Appl. Physiol.*, 89(2):840–847, 2000.

[48] RE Taylor, C Zheng, RP Jackson, JC Doll, JC Chen, KRS Holzbaur, T Besier, and E Kuhl. The phenomenon of twisted growth: humeral torsion in dominant arms of high performance tennis players. *Comp. Methods Biomech. Biomed. Eng.*, 12(1):83–93, 2009.

[49] MP Coutts and John Grace. *Wind and trees*. Cambridge University Press, 1995.

[50] Eugene E Berg. Chinese foot binding. *Orthopaedic Nursing*, 14(5):66–69, 1995.

[51] G. R. Cramer and D. C. Bowman. Kinetics of maize leaf elongation. I. Increased yield threshold limits short-term, steady-state elongation rates after exposure to salinity. *J. Exp. Bot.*, 42(244):1417–1426, 1991.

[52] D. Bray. Axonal growth in response to experimentally applied mechanical tension. . *Dev. Biol.*, 102(2):379, 1984.

[53] J. Zheng, P. Lamoureux, V. Santiago, T. Dennerll, R. E. Buxbaum, and S. R. Heidemann. Tensile regulation of axonal elongation and initiation. *J. Neurosci.*, 11:1117–1125, 1991.

[54] Phillip Lamoureux, Gordon Ruthel, Robert E Buxbaum, and Steven R Heidemann. Mechanical tension can specify axonal fate in hippocampal neurons. *J. Cell Biol.*, 159(3):499–508, Nov 2002.

[55] S. R. Heidemann, P. Lamoureux, and R. E. Buxbaum. Cytomechanics of axonal development. *Cell Biochem. Biophys.*, 27(3):135–155, 1997.

[56] R. Thoma. *Untersuchungen über die Histogenese und Histomechanik des Gefäßsystems*. Enke, 1893.

[57] C. L. Berry. The growth and development of large arteries. *Exp. Embryol. Teratology*, 1:34–64, 1974.

[58] L. A. Taber. An optimization principle for vascular radius including the effects of smooth muscle tone. *Biophys. J.*, 74(1):109–114, 1998.

[59] S. Lehoux, Y. Castier, and A. Tedgui. Molecular mechanisms of the vascular responses to haemodynamic forces. *J. Intern. Med.*, 259(4):381–392, 2006.

[60] R. L. Gleason and J. D. Humphrey. Effects of a sustained extension on arterial growth and remodeling: a theoretical study. *J. Biomech.*, 38(6):1255–1261, 2005.

[61] R. H. Woods. A few applications of a physical theorem to membranes in the human body in a state of tension. *Trans. Roy. Acad. Med. Ireland*, 10(1):417–427, 1892.

[62] S Marsh Tenney. A tangled web: Young, Laplace, and the surface tension law. *Physiology*, 8(4):179–183, 1993.

[63] Ronald R Martin and Howard Haines. Application of Laplace's law to mammalian hearts. *Comp. Biochem. Physiol.*, 34(4):959–962, 1970.

[64] Alan C Burton. The importance of the shape and size of the heart. *American Heart J.*, 54(6):801–810, 1957.

[65] V. Kumar, A. K. Abbas, N. Fausto, and J. C. Aster. *Robbins & Cotran pathologic basis of disease*. Elsevier Health Sciences, 2009.

[66] W. Mueller-Klieser, S. Schreiber-Klais, S. Walenta, and MH Kreuter. Bioactivity of well-defined green tea extracts in multicellular tumor spheroids. *Int. J. Oncol.*, 21(6):1307–1315, 2002.

[67] R. M. Sutherland. Cell and environment interactions in tumor microregions: the multicell spheroid model. . *Science*, 240(4849):177, 1988.

[68] M. T. Santini and G. Rainaldi. Three-dimensional spheroid model in tumor biology. *Pathobiology*, 67(3):148–157, 2000.

[69] A. J. Franko and H. I. Freedman. Model of diffusion of oxygen to spheroids grown in stationary medium—I. Complete spherical symmetry. *Bull. Math. Biol.*, 46(2):205–217, 1984.

[70] G. Helmlinger, P. A. Netti, H. C. Lichtenbeld, R. J. Melder, and R. K. Jain. Solid stress inhibits the growth of multicellular tumor spheroids. *Nature Biotech.*, 15:778–783, 1997.

[71] Richard S Cowan. *A monograph of the genus Eperua (Leguminosae-Caesalpinioideae)*. Smithsonian Institution Press Washington, DC, 1975.

[72] P. Détienne and J. Thiel. Monographie des Wapas de Guyane Française. *Bois For. Trop.*, 216:43–68, 1988.

[73] W. S. Peters and D. A. Tomos. The epidermis still in control. *Acta Botanica*, 109:264–267, 1996.

[74] R. Skalak, S. Zargaryan, R. K. Jain, P. A. Netti, and A. Hoger. Compatibility and the genesis of residual stress by volumetric growth. *J. Math. Biology*, 34:889–914, 1996.

[75] R. Skalak. Growth as a finite displacement field. In D. E. Carlson and R. T. Shield, editors, *Proceedings of the IUTAM Symposium on Finite Elasticity*. Martinus Nijhoff, The Hague, 1981.

[76] C. S. Gager. *Fundamentals of Botany*. P. Blakiston's Son & Co., 1916.

[77] G. F. Atkinson. *Lessons in Botany*. Henry Holt and Company. New York, 1900.

[78] N. J. C. Müller. *Handbuck der botanik*. Heidelberg, 1880.

[79] U. Kutschera. Tissue stresses in growing plant organs. *Physiol. Plantarum*, 77:157–163, 1989.

[80] J. Bonner. The action of the plant growth hormone. *J. Gen. Physiol.*, 17(1):63–76, 1933.

[81] R. K. Bamber. A general theory for the origin of growth stresses in reaction wood: how trees stay upright. *IAWA J.*, 22(3):205–212, 2001.

[82] RD Firn and J. Digby. The role of the peripheral cell layers in the geotropic curvature of sunflower hypocotyls: a new model of shoot geotropism. *Aust. J. Plant Physiol.*, 4:337–347, 1977.

[83] K. V. Thimann and C. L. Schneider. Differential growth in plant tissues. *Am. J. Bot.*, 25(8):627–641, 1938.

[84] Y. C. Fung. What principle governs the stress distribution in living organs? In Y. C. Fung, E. Fukada, and J. J. Wang, editors, *Biomechanics in China, Japan and USA*, pages 1–13. Science Press, Beijing, 1983.

[85] Y. C. Fung. What are the residual stresses doing in our blood vessels? *Ann. Biomed. Eng.*, 19(3):237–249, 1991.

[86] Y. C. Fung. *Biomechanics: mechanical properties of living tissues*. Springer, New York, 1993.

[87] A. Rachev. Theoretical study of the effect of stress-dependent remodeling on arterial geometry under hypertensive conditions. *J. Biomech.*, 30:819–827, 1997.

[88] G. A. Holzapfel, M. Stadler, and C. A. J. Schulze-Bauer. A layer-specific three-dimensional model for the simulation of balloon angioplasty using magnetic resonance imaging and mechanical testing. *Ann. Biomed. Eng.*, 30(6):753–767, 2002.

[89] D. H. Bergel. *The visco-elastic properties of the arterial wall.* PhD thesis, University of London, 1960.

[90] H. Gregersen, GS Kassab, and YC Fung. Review: The zero-stress state of the gastrointestinal tract. *Digest. Dis. Sci.*, 45(12):2271–2281, 2000.

[91] E. U. Azeloglu, M. B. Albro, V. A. Thimmappa, G. A. Ateshian, and K. D. Costa. Heterogeneous transmural proteoglycan distribution provides a mechanism for regulating residual stresses in the aorta. *Am. J. Physiol. -Heart C.*, 294(3):H1197–H1205, 2008.

[92] JH Omens, AD McCulloch, and JC Criscione. Complex distributions of residual stress and strain in the mouse left ventricle: experimental and theoretical models. *Biomech. Model. Mechanobiol.*, 1(4):267–277, 2003.

[93] HC Han and YC Fung. Residual strains in porcine and canine trachea. *J. Biomech.*, 24(5):307–309, 1991.

[94] G. Xu, P. V. Bayly, and L. A. Taber. Residual stress in the adult mouse brain. *Biomech. Model. Mechanobiol.*, 8(4):253–262, 2009.

[95] Bijay Giri, Shigeru Tadano, Kazuhiro Fujisaki, and Masahiro Todoh. Understanding site-specific residual strain and architecture in bovine cortical bone. *J. Biomech.*, 41(15):3107–3115, 2008.

[96] L. V. Beloussov, J. G. Dorfman, and V. G. Cherdantzev. Mechanical stresses and morphological patterns in amphibian embryos. *J. Embryol. Exp. Morph.*, 34(3):559–574, 1975.

[97] D. Ambrosi and F. Mollica. The role of stress in the growth of a multicell spheroid. *J. Math. Biol.*, 48:477–499, 2004.

[98] S. J. Kowalski and A. Rybicki. Residual stresses in dried bodies. *Dry. Technol.*, 25(4):629–637, 2007.

[99] J. Lepetit, P. Salé, and A. Ouali. Post-mortem evolution of rheological properties of the myofibrillar structure. *Meat Sci.*, 16(3):161–174, 1986.

[100] FH Cilley. Fundamental propositions in the theory of elasticity; a study of primary or self-balancing stresses. *Amer. J. Sci.*, 11(64):269–290, 1901.

[101] YC Tsui and TW Clyne. An analytical model for predicting residual stresses in progressively deposited coatings part 1: Planar geometry. *Thin Solid Films*, 306(1):23–33, 1997.

[102] P. J. Withers. Residual stress and its role in failure. *Rep. Prog. Phys.*, 70(12):2211–2264, 2007.

[103] B. Giri, K. Fujisaki, M. Todoh, and S. Tadano. Residual stress estimation of bone tissue using X-ray imaging technique. *J. Biomech.*, 40(2):371, 2007.

[104] A. Goriely and M. Ben Amar. On the definition and modeling of incremental, cumulative, and continuous growth laws in morphoelasticity. *Biomech. Model. Mechanobiol.*, 6(5):289–296, 2007.

[105] A. Goriely and D. E. Moulton. Morphoelasticity - a theory of elastic growth. In Oxford University Press, editor, *New Trends in the Physics and Mechanics of Biological Systems*, 2010.

[106] M. Ben Amar and A. Goriely. Growth and instability in elastic tissues. *J. Mech. Phys. Solids*, 53:2284–2319, 2005.

[107] A. Goriely, R. Vandiver, and M. Destrade. Nonlinear Euler buckling. *Proc. Roy. Soc. Lond. A*, 464(2099):3003–3019, 2008.

[108] A. Goriely and R. Vandiver. On the mechanical stability of growing arteries. *IMA J. Appl. Math.*, 75(4):549–570, 2010.

[109] J. Dervaux and M. Ben Amar. Morphogenesis of growing soft tissues. *Phys. Rev. Lett.*, 101(6):068101, 2008.

[110] A. J. Franko and R. M. Sutherland. Oxygen diffusion distance and development of necrosis in multicell spheroids. *Radiat. Res.*, pages 439–453, 1979.

[111] J. P. Freyer, N. H. Fink, P. L. Schor, J. R. Coulter, M. Neeman, and L. O. Sillerud. A system for viably maintaining a stirred suspension of multicellular spheroids during NMR spectroscopy. *NMR Biomed.*, 3:195–205, 1990.

[112] HP Greenspan. Models for the growth of a solid tumor by diffusion. *Stud. Appl. Math.*, 51(4):317–340, 1972.

[113] Y. Kim, M. A. Stolarska, H. G. Othmer, N. Bellomo, and PK Maini. A hybrid model for tumor spheroid growth in vitro I: Theoretical development and early results. *Math. Model. Meth. Appl. Sci.*, 17:1773, 2007.

[114] P. Macklin, S. McDougall, A. R. A. Anderson, M. A. J. Chaplain, V. Cristini, and J. Lowengrub. Multiscale modelling and nonlinear simulation of vascular tumour growth. *J. Math. Biol.*, 58:765–798, 2009.

[115] G. Hamilton. Multicellular spheroids as an in vitro tumor model. *Cancer Lett.*, 131(1):29–34, 1998.

[116] E. K. Rodriguez, A. Hoger, and A. McCulloch. Stress-dependent finite growth in soft elastic tissue. *J. Biomech.*, 27:455–467, 1994.

[117] G. A. Holzapfel. Biomechanics of soft tissue. *The handbook of materials behavior models*, 3:1049–1063, 2001.

[118] A Mallock. Note on the instability of india-rubber tubes and balloons when distended by fluid pressure. *Proc. Roy. Soc. Lond.*, 49(296-301):458–463, 1890.

[119] W. A. Osborne and W Sutherland. The elasticity of rubber balloons and hollow viscera. *Proc. Roy. Soc. Lond. B*, 81(551):485–499, 1909.

[120] R. W. Ogden. *Non-linear Elastic Deformations*. Dover, New york, 1984.

[121] M. E. Gurtin. *An introduction to continuum mechanics*. Academic Press, 1981.

[122] C. Truesdell and W. Noll. *The Non-Linear Field Theories of Mechanics*. Springer, 2004.

[123] D. K. Bogen and Th A. McMahon. Do cardiac aneurysms blow out? *Biophys. J.*, 27, 1979.

[124] O. A. Shergold, N. A. Fleck, and D. Radford. The uniaxial stress versus strain response of pig skin and silicone rubber at low and high strain rates. *Int. J. Impact Eng.*, 32:1384–1402, 2006.

[125] A. N. Gent. Elastic instabilities in rubber. *Int. J. Non-Linear Mech.*, 40:165–175, 1995.

[126] A. Gent. A new constitutive relation for rubber. *Rubber Chem. and Technol.*, 69, 1996.

[127] C. O. Horgan and G. Saccomandi. Constitutive modeling of rubber-like and biological materials with limited chain extensibility. *Math. Mech. Solids*, 7:353–371, 2002.

[128] C. O. Horgan and G. Saccomandi. A description of arterial wall mechanics using limiting chain extensibility constitutive models. *Biomech. Model. Mechanobiol.*, 1, 2003.

[129] G. A. Holzapfel, T. C. Gasser, and R. W. Ogden. A new constitutive framework for arterial wall mechanics and a comparative study of material models. *J. Elasticity*, 61:1–48, 2000.

[130] A. Delfino, N. Stergiopulos, J. E. Moore, and J. J. Meister. Residual strain effects on the stress field in a thick wall finite element model of the human carotid bifurcation. *J. Biomech.*, 30(8):777–786, 1997.

[131] L. Horny, J. Kronek, H. Chlup, E. Gultova, L. Heller, R. Zitny, and D. Vokoun. Inflation-extension test of silicon rubber-nitinol composite tube. In *5th European Conference of the International Federation for Medical and Biological Engineering*, pages 1027–1030. Springer, 2012.

[132] D. Bigoni and M. Gei. Bifurcations of a coated, elastic cylinder. *Int. J. Solids Struct.*, 38(30-31):5117–5148, 2001.

[133] J. Dolbow, E. Fried, and H. Ji. Chemically induced swelling of hydrogels. *J. Mech. Phys. Solids*, 52(1):51–84, 2004.

[134] C. J. Chuong and Y. C. Fung. Three-dimensional stress distribution in arteries. *J. Biomech. Eng.*, 105:268–274, 1983.

[135] D. Ambrosi and F. Guana. Stress-modulated growth. *Math. Mech. Solids*, 12(3):319–342, 2007.